

EFFECT OF OXIDATIVE STRESS ON HUMAN TELOMERIC DNA STRUCTURAL
DYNAMICS AND ACCESSIBILITY

BY

GRACE SOOYEON KIM

THESIS

Submitted in partial fulfillment of the requirements
for the degree of Master of Science in Bioengineering
in the Graduate College of the
University of Illinois at Urbana-Champaign, 2014

Urbana, Illinois

Adviser:

Assistant Professor Sua Myong

ABSTRACT

The ends of human telomeric DNA consist of single-stranded overhangs of tandem TTAGGG repeats (ssTEL) that can form into a G-quadruplex (GQ). This guanine-rich sequence is prone to 8-oxoguanine (8OG) damage, which is one of the most common oxidative DNA lesions that can compromise telomere integrity. Here, we use single molecule Förster Resonance Energy Transfer (smFRET) to characterize the effect of 8OG on the structural dynamics and accessibility of ssTEL. We show that the stable GQ folding observed in ssTEL is disrupted by a single 8OG, generating dynamic conformational fluctuations of the DNA. Such structural dynamics induced by 8OG lead to increased binding of complementary DNA oligonucleotides, as well as faster and more effective association of a telomere binding protein, protection of telomeres 1 (POT1), suggesting enhanced accessibility of telomeric DNA to interacting molecules. The increased dynamics and accessibility caused by 8OG is comparable to the effect of a base substitution from G to C at the same position, which abolishes the Hoogsteen basepairing required for GQ folding. Our results suggest that a single 8OG in telomeric DNA can lead to destabilization of GQ folding, which may alter the processes that govern telomere maintenance and extension activity.

ACKNOWLEDGMENTS

First, I thank my advisor, Sua Myong, for her guidance and mentorship. I will always be grateful for the patience and generosity she has shown, even in the midst of the personal struggles I faced while in her lab, and for the opportunity to rebuild and learn some of the most valuable lessons I needed to grow personally and professionally.

I thank Patricia Opresko (University of Pittsburgh) for generously providing the recombinant human POT1 protein, and Noah Buncher, from her lab, who purified the protein.

I would like to express my gratitude to the lab members who reside in DCL: Ramreddy Tipanna and Alex Kreig, the in-house GQ specialists, who especially taught me single molecule experiment prep; (Peggy) Yupeng Qiu, who taught me how to use the TIRF scope and run smFRET measurements; and Younghoon Kim, who especially advised me on data processing and analysis. Special thanks to Hye Ran Koh for making her expertise readily available, especially when setting up the shutter control for ALEX. And, of course, a very special thanks to Helen Hwang, the original in-house telomere authority, who made herself available to answer any questions, despite having been in the midst of M2 madness. I am grateful for the special friendship I have enjoyed with each lab member, and cannot go without mentioning Shirley Wang, whose constancy, thoughtfulness, and levelheadedness was a unique source of encouragement and support, and our recently joined postdoc, Huiting Lee, for fun conversations.

Support outside of lab played just as important of a role in the completion of this project. To name a few key players: Nora Few, for her guidance, backing, and sanity support; Wendy Evans, for her well-informed advice, perspective, confidence, and non-judgment, despite having witnessed, up close, the peak of my neuroticism; Olivia Cangellaris, for her dedicated presence in the form of imgur links, delivered food, and checkpoints through daily decision making processes; the classified VIPs who keep tabs on me, listen to my rants, give me counsel I would rather not hear, and make sure I have a good time during my occasional escapes from Champaign; and finally, my bratty, yet charming, sister Theresa, and my parents, Irene and Thomas, for their unconditional love, encouragement, and presence.

Financial support for this work was provided by the National Institute of Health (1DP2GM105453) and the American Cancer Society (RSG-12-066-01-DMC).

TABLE OF CONTENTS

| | |
|--|-----------|
| CHAPTER 1: INTRODUCTION..... | 1 |
| CHAPTER 2: MATERIALS AND METHODS | 20 |
| CHAPTER 3: RESULTS AND DISCUSSION | 23 |
| CHAPTER 4: CONCLUSION..... | 29 |
| FIGURES AND TABLES | 30 |
| REFERENCES..... | 42 |

CHAPTER 1: INTRODUCTION

1.1 Structure and Properties of G-quadruplex

The structure of the G-quadruplex was first identified by Gellert et al. (1962) in order to determine why guanosine has the unusual physical property of being able to form gels readily in aqueous solution (1). Based on diffraction patterns, they postulated that the guanosine monophosphate (GMP) gel fibers had a regular helical structure with a hydrogen bonding arrangement of four coplanar guanine bases, which act as both a donor and acceptor of two hydrogen bonds between each Hoogsteen G-G base pair. They also predicted that these G-quartet structure could stack on top of each other to form linear aggregates, which are now known as G-quadruplex (GQ) or G-tetraplex.

Further studies revealed that monovalent cations are needed in the central cavity of GQs to complex with inwardly projecting carbonyl oxygens (guanine O6), in order to neutralize electrostatic repulsion (2, 3). They determined that the binding capacity is size-specific, and calculated that Li^+ is too small to form a complex, Na^+ fits easily in the center of the plane, and that K^+ is too large to fit in the plane, but can fit between two planar tetramers, thus promoting GQ stability most efficiently (4–6).

Although the structure of GQ is primarily determined by the condensation of guanine residues around this monovalent cation, secondary effects such as base-stacking forces, hydrogen bonding, and hydrophobic effects determine the final structure (7). As a result, the stability, kinetics, and conformation of GQ are very sensitive to multiple factors, such as ionic conditions, temperature, molecular crowding conditions, strand stoichiometry, and DNA length, sequence, arrangement, and concentration (4–6, 8–16). Under these conditions, the structural polymorphism of GQ can be classified by molecularity: intramolecular (one strand) or intermolecular (two or more strands), strand orientation: anti-parallel, parallel, or hybrid (between anti-parallel and parallel), guanine glycosidic angles: *syn* or *anti* conformations, and loop orientation: lateral, diagonal, or propeller (17). The strand orientation and guanine conformation are interrelated in that all parallel GQs have all guanine glycosidic angles in an *anti* conformation, while anti-parallel GQs have both *syn* and *anti* guanines (17).

The structural polymorphism and folding pathways of various GQ structures are relevant to understanding the context and scope of GQ studies, and can be illustrated by the various

intramolecular GQ structures seen in human telomeric DNA (11–26). This property has implications for the design of GQ binding ligands, which have potential in cancer therapeutics among many other applications.

1.2 Evidence for Biological Functions of DNA G-quadruplex

Two bioinformatics studies applying different algorithms concurrently reached similar conclusions of ~375,000 (27) and ~376,000 (28) candidate sequences with tracts of tandem guanines that may form intramolecular DNA GQs in the human genome. Of these, 60% (~223,000) were found in intergenic regions, 40% (~151,000) within genes, and only ~14,000 within exons (27). Huppert & Balasubramanian (2005) also noted the significant repression of GQs in the coding strand of exons, and suggested that there may be evolutionary pressure to reduce the number of GQs allowed to form in mRNA (28).

More detailed analyses in regulatory regions have shown that GQ motifs are concentrated in promoter regions with the frequency increasing closer to transcription start sites (29). In fact, nearly half of all known genes in the human genome contain such putative GQ sequences within a 1,000 nucleotides upstream of transcription start sites (29). Studies that correlated GQ formation with functional classes of genes found that promoters of housekeeping and tumor suppressor genes are under-represented in GQ motifs, while promoters of human oncogenes and regulatory genes (e.g., transcription factors) are over-represented (29, 30). This suggests that genomic structure undergoes selection based on gene function, and that this may be a mechanism for global regulation of gene expression.

Early *in vivo* studies focusing on single genes suggested the presence of GQ structures in important regulatory regions and postulated biologically relevant roles for these secondary structures. Subsequent studies provided evidence supporting their hypotheses and also determined possible mechanisms for these biological functions.

In the late 1980s, intramolecular GQs were found in single stranded telomeric DNA and were predicted to influence telomere functioning (31–33). Since then, many studies have further studied telomeric GQ folding conformations and dynamics (11, 12, 18–26, 34) and provided evidence for the various roles of telomeric GQ in telomere maintenance. One of the most well studied functions is the inhibitory effect of GQ on telomerase-based telomere lengthening (35).

This observation is the basis for development of GQ stabilizers as an anticancer therapeutic (36). The effect of GQ on telomeres will be discussed in further detail in later sections.

Other early findings suggested the involvement of GQ in transcriptional regulation. GQs were found in a regulatory region upstream of the insulin gene (37), the 5' sequence of human and mouse retinoblastoma susceptibility genes (38), and a nuclease-hypersensitive element upstream of a promoter of the human c-MYC proto-oncogene (39, 40). Siddiqui-Jain et al. (2002) studied the structure and function of GQ in this particular c-MYC promoter region, and found that it acts as a repressor of c-MYC transcription. They showed that a GQ binding ligand suppresses c-MYC transcription, while a single point mutation that destabilizes the GQ structure results in a 3-fold increase in basal transcriptional activation (41).

It is thought that GQ structures both positively and negatively regulate transcription (42). GQs on the template strand can inhibit transcription, while those on the non-template strand can enhance transcription by maintaining the transcribed strand in a single-stranded conformation. GQ-protein interactions may also modulate transcription, based on the nature of the protein. Genome-wide analysis of the effect of a GQ binding ligand found that expression levels of many genes were both up and down regulated (43). Another genome-wide study investigated the effects of GQ unwinding helicases on transcription and determined that Werner's syndrome (WRN) or Bloom's syndrome (BLM) helicase deficiency significantly upregulates genes associated with GQ motifs, which account for 20-30% of genes upregulated (44).

Various studies have also demonstrated the recombinogenic potential of GQ structures. Sen & Gilbert (1988) suggested that GQ is involved in synapsis during meiosis and that it is responsible for switch recombination at G-rich human immunoglobulin heavy-chain switch regions, which allows for antibody diversity (4). Larson et al. (2005) then provided evidence for this by showing that MutS α , a DNA mismatch repair protein, binds with high affinity to GQ structures that form upon transcription of intronic, G-rich, and repetitive switch regions (45). This event then promotes DNA synapsis and activates switch recombination. Another study in *Neisseria gonorrhoeae* found that a single GQ sequence in the recombination initiation sequence is necessary to promote antigenic variation of its surface epitopes (46). They found that GQ-disrupting mutations and GQ stabilization both prevented DNA nicks within the GQ region and blocked antigenic variation, which allows the pathogen to avoid detection by the host immune

system (46). In a later study, they showed that inactivating the promoter of a small non-coding RNA that initiates within the GQ forming sequence, blocks antigenic variation (47).

Homologous recombination (HR) is an important mechanism for double-stranded DNA break (DSB) repair in mammalian cells, and is also known to promote the restart and repair of stalled or broken replication forks (48). Replication forks that stall at GQ motifs may become remodeled into recombination intermediates, which suggests that stalled replication or DNA breakage near GQs can be rescued by recombination (49, 50).

The significant colocalization of GQ motifs with sites susceptible to breakage (51), implicates GQ structures in hindering transcription and replication (44), which are processes that require accessibility and readability of each base to faithfully transmit genetic information. This is supported by evidence that GQ stabilizers induce DNA breaks and affect expression of genes that have GQs in their promoter regions (51–54), and by evidence that helicases prevent DNA damage by resolving GQ structures during DNA replication (44, 53, 55–57).

Of note, human helicases that unwind GQ are associated with human diseases that cause genomic instability, including Werner's syndrome (WRN), which is associated with premature aging, Bloom's syndrome (BLM), which is associated with increased cancer risk, and Fanconi anemia (FANCF) and PIF1, which are both also associated with predisposition to cancer (42, 58). Interestingly, these helicases can counter GQ barriers at replication forks, as well as repair DSBs (44, 53, 59–61), which highlights their importance for suppressing genome instability.

London et al. (2008) provided strong evidence that human disease is associated with a loss of GQ unwinding by mapping the accumulation of large genomic deletions at GQ containing regions in a FANCF-deficient human cell line (61). Similarly, studies in *Caenorhabditis elegans* showed that mutation in the DOG-1 helicase, which is distantly related to FANCF, causes genome-wide deletions in putative GQ forming sequences (62, 63). Rodriguez et al. (2012) demonstrated that the GQ stabilizer, pyridostatin, bound preferentially to GQ motifs genome-wide and caused replication and transcription-dependent DNA damage, which then induced growth arrest in human cancer cells. They used chromatin immunoprecipitation sequence (ChIP-Seq) analysis to detect high DNA damage marker (γ H2Ax) content in regions with putative GQ sequences, which colocalized with PIF1 foci in pyridostatin-treated human cells. Additionally, Koole et al. (2014) also discovered a profound loss of GQ surrounding sequences in the absence

of the A-family polymerase Theta, which is necessary for a non-canonical DNA break repair mechanism that prevents genomic instability and replication fork barriers (64).

The GQ barrier at the DNA replication fork may also interfere with the inheritance of epigenetic information. The propagation of histone marks is thought to rely on local recycling of parental histones to nascent daughter DNA strands (65), and subsequent copying of the epigenetic state of the parental DNA to newly deposited histones, during DNA replication. The lack of REV1 translesion polymerase causes genome-wide dysregulation of gene expression, which is correlated with altered histone marks nearby GQ motifs (66). This suggests a disturbance in GQ-dependent transcription and maintenance of epigenetic integrity. The effect is even more prominent when FANCI, WRN, and BLM helicases are deficient (67, 68).

Despite these studies, there has been debate as to whether these structures existed and had functional roles in living cells. One of the first studies to provide direct evidence for the existence of GQ *in vivo* detected parallel telomeric GQs from a ciliate (*Stylonychia lemnae*) using antibody staining (69). Another study that established GQ DNA formation *in vivo* was done by introducing a plasmid containing human telomeric repeat inserts in E.coli and inducing transcription in these living cells to observe the formation of intramolecular GQ DNA using electron microscopy (70). Müller et al. (2010) also provided direct evidence for the existence of GQ in telomeric DNA by using a small molecule GQ binding ligand that targets telomeric GQ structures to pull down telomeric DNA (71).

More recent studies have developed GQ specific antibodies and ligands to use them for visualizing GQ structures in human cells and for isolating GQ forming sequences from human genomic DNA. Henderson et al. (2013) developed monoclonal antibodies specific for different GQ DNA structures and identified one that exhibited strong nuclear staining in mammalian cells (72). They showed that nuclear staining intensity increased when cells were treated with GQ binding ligands or when they were deficient in FANCI, which is a GQ DNA-specific helicase that unwinds GQ structures. Lam et al. (2013) confirmed the existence and stability of GQ structures in human genomic DNA, by using another engineered antibody to pull-down GQ structures and conducting deep sequencing to detect and map GQ at a high resolution (73). They found stable GQ structures in sub-telomeres, gene bodies, and gene regulatory regions, and showed that GQ stabilizing small molecules can modulate transcription in identified GQ containing genes. Biffi et al. (2013) followed the formation of GQ structures during cell cycle

progression and found that it is formed during DNA replication, and is resolved when cellular processes are quiescent and no replication occurs (74). They also applied pyridostatin to confirm that small molecule ligands interact directly with endogenous DNA and stabilize GQ structures (74), which may then lead to DNA damage if not resolved (54).

Early studies suggesting the existence of DNA GQ structures in important regulatory regions were followed by findings that provided evidence for their biological relevance. Complementary bioinformatics studies revealed the non-random abundance of GQ motifs in these genomic regions, which include telomeres, oncogenic gene promoter regions, and recombination hotspots. The existence of proteins that bind, cleave, resolve or promote formation of GQ has provided compelling evidence for the *in vivo* relevance of GQ. Likewise, the discovery and development of GQ binding ligands and antibodies have allowed *in vivo* experiments to examine dysregulation of DNA processes by GQ stabilization, directly visualize GQ structures in cells, and isolate GQ forming sequences from genomic DNA. In conclusion, DNA GQ structures have emerged as a significant player in telomere maintenance, transcriptional regulation, DNA recombination, DNA replication, DNA repair, and epigenetic regulation.

1.3 Overview of Telomeres and their Processes

In the 1930s, Hermann Müller and Barbara McClintock were the first to observe that chromosome ends were not prone to degradation, recombination, and end-to-end fusions (75, 76). Their cytogenetic studies were confirmed by Sandell & Zakian (1993), who used yeast strains to show that eliminating this protected end, coined telomere by Müller, resulted in RAD9-mediated cell cycle arrest and a dramatic loss of telomeres (77). They determined that telomeres prevent the ends from being recognized as double-stranded DNA breaks (DSBs) by DNA damage machinery.

Studies in various eukaryotes found that telomeric DNA is highly conserved and share a common feature of GC rich tandem repeat sequences (78–83). In vertebrates, telomeric DNA was determined to extend beyond the DNA duplex to form a terminal 3' single-stranded G-overhang (ssTEL) of varying lengths (84, 85). In humans, the telomeric DNA consists of 5'-TTAGGG-3' hexameric repeats (83), and is about 150 to 200 nucleotides long (86, 87).

Telomeric DNA has been observed to adopt two different protective forms that sequester the ssTEL: the T-loop structure, where ssTEL folds back and invades into the double-stranded DNA (D-loop) (88), and the intramolecular G-quadruplex structure (GQ) (31, 32, 69). These capping structures are thought to represent different functional states, but may not be mutually exclusive (16, 89).

In addition to chromosome end protection, telomeres are involved in preventing important genetic information from being lost. These non-coding repeat sequences serve as an expendable buffer that gets shortened with each round of DNA replication, which occurs due to the inability of DNA polymerase to completely replicate DNA ends. This end-replication problem is resolved by a telomere lengthening mechanism (90, 91).

The first to be discovered and garner a great deal of attention is a mode of telomere replication that involves telomerase. Greider and Blackburn identified an enzyme in *Tetrahymena* ciliates that could synthesize tandem telomere repeats *de novo* using deoxynucleoside triphosphate substrates (dNTPs), without using ATP (78, 92). They determined that the specialized ribonucleoprotein complex needed both its reverse transcriptase enzyme and RNA template (93, 94), and developed the telomerase elongation model where telomerase base pairs complementary sequences at the 3' tail to its RNA template, adds a repeat sequence, translocates, and continues this process (75).

However, telomerase is differentially expressed, and this is thought to contribute to heterogeneity in telomere length. Observations of telomere length in different human tissues suggested that telomerase is active in germline cells, but not in somatic cells (75). Normal somatic human cells progressively lose telomeres with each round of DNA replication until their telomeres reach a critically short length, the “Hayflick limit”, after which they respond by entering a senescent state (95, 96). If they continue to divide they enter crisis, which leads to progressive chromosomal instability and apoptosis, as is seen in aging (91, 97, 98).

Cancer cells overcome senescence and crisis, and hijack a telomere lengthening mechanism to acquire unlimited replicative potential, which enables them to divide indefinitely and transform into immortalized cells. This immortalization is a critical step in tumorigenesis and is considered one of the hallmarks of cancer (99).

Most cancer cells (~85%), typically carcinomas, do this by overexpressing telomerase (100). Transformation of cells by oncogenes or ectopic expression of the human telomerase

reverse transcriptase (hTERT), both activated telomerase and stabilized telomere length to allow postsenescent cells to proliferate beyond crisis (101, 102). These methods were used to directly convert normal human epithelial and fibroblast cells into cancer cells (103). Conversely, inhibition of telomerase activity by expression of mutant telomerase was shown to reduce telomere length and cause death of tumor cells (104).

By contrast, ~10-15% of cancers, which include many sarcomas and glioblastoma multiforme, were found to maintain telomere length by the alternative lengthening of telomeres (ALT) pathway (105), which involves recombination-mediated DNA replication (106–110). This form of DNA replication can be achieved by copying telomeric sequences between sister chromatids or by loop-mediated copying. Dunham et al. (2000) showed that DNA sequences can be copied from telomere to telomere by homologous recombination and copy switching (109), while Muntoni et al. (2009) revealed that intra-telomeric DNA copying can also occur when primed by a t-loop structure (111). The fact that human ALT cells have abundant telomeric circles, points to frequent t-loop homologous recombination events that can promote rolling circle replication of telomeres (112).

Murnane et al. (1994) followed human ALT+ cells undergoing steady telomere attrition and then suddenly having a change in telomere length, which suggests recombination (113). As a result, ALT+ cells are characterized by variable telomere lengths, which is in contrast to telomerase-positive cells that generally maintains a stable and homogeneous telomere length (108, 114). Yeager et al. (1999) also discovered the ALT-associated PML bodies (APBs), which are large subnuclear complexes where PML bodies colocalize with telomeric DNA, telomeric binding proteins, and proteins involved in DNA synthesis and recombination, such as RAD51 and RAD52 (115). APBs are considered to be one of the hallmarks of the ALT mechanism and has been found to appear as soon as ALT is activated (115). Additionally, ALT+ cells generate telomeres with variant repeat sequences due to recombination events with upstream subtelomeric sequences (116), and have telomeres that spontaneously elicit a DNA damage response (DDR), but repress fusions (117). Cesare & Reddel (2010) suggested that these telomeres can adopt three distinct states with various levels of chromosome end protection: a “closed-state” that represses DDRs and fusions, an “intermediate-state” that is susceptible to DDR but repress fusions, and an “uncapped” state that is susceptible to both (118). They speculate that DSB

repair proteins localize to intermediate telomeres, but actively prevent fusions by shelterin proteins, most likely TRF2 and RAP1, which are known to inhibit these events.

In mammals, the shelterin complex is essential for telomere regulation and protection, as well as control of signaling cascades from the chromosome ends. It consists of six proteins: POT1 (protection of telomeres 1), TPP1 (POT1-interacting protein 1, formerly PIP1), TIN2 (TRF1 interacting nuclear factor 2), TRF1 (telomeric repeat binding factor 1), TRF2 (telomeric repeat binding factor 2), and RAP1 (repressor/activator protein 1) (119). In humans, the shelterin complex may interact with ~200 other telomere-associated proteins that may also influence telomeric structure (120). Of the six proteins that make up the shelterin complex, POT1 protein binds specifically to ssTEL. It forms a heterodimer with TPP1, which links it to the other shelterin proteins and to telomerase, and also with TRF2, which binds telomeric double-stranded DNA (121).

The interaction between POT1 and TRF1 via TPP1 and TIN2, allows POT1 to transduce information about telomere length to the telomere terminus, where telomerase is regulated, and also allows TRF1 to regulate POT1 binding/loading on ssTEL in response to telomere length (122, 123). Kendellen et al. (2009) reported that association of POT1 with TRF2 is also critical for telomere length homeostasis (124).

In addition to being involved with regulating telomere length, POT1 binds to the 3' end of ssTEL to prevent unwanted DNA damage response (121, 125–133). Its ssDNA binding domain dictates ssTEL recognition and is a conserved DNA-binding motif, known as an (oligonucleotide/oligosaccharide binding) OB-fold (134). Lei et al. (2004) reported the crystal structure of the DNA binding domain of human POT1 (hPOT1) bound to the minimum binding sequence of 5'-TTAGGGTTAG-3', which is about one and a half telomere repeats (135). They revealed that two tandem OB folds pack together and form a continuous binding cleft. The N-terminal OB fold of hPOT1 binds to the first six nucleotides, while the second OB fold binds and protects the 3' end of ssTEL. Of note, the last nucleotide G10 is deeply buried in the binding pocket of the second OB fold, which may be involved in preventing access by telomerase (135).

Studies of each OB fold in mouse paralogs, Pot1a and Pot1b, showed that both OB folds of POT1 are necessary for suppression of DNA damage response and proper maintenance of chromosomal stability (128, 129, 131). Bunch et al. (2005) determined that reduction of POT1 first results in telomere lengthening, but after further reduction, triggers loss of telomeric DNA

and end-to-end fusions (136). This suggests that the amount of telomere bound POT1 determines differential outcomes *in vivo*.

In conclusion, telomeres are specialized DNA-protein complexes that safeguard genomic integrity by protecting the ends of linear eukaryotic chromosomes and by replenishing its own DNA as a solution to counteract the end-replication problem. They prevent the 3' termini from being recognized as double-stranded DNA breaks by DNA repair machinery and regulate its access to various telomere binding proteins, including those involved in regulating telomerase-based extension and the ALT pathway. Its dysfunction leads to degradation by nuclease attack, unwanted recombination, telomere damage induced foci (TIF), end-to-end fusions, and ultimately leads to cell cycle arrest, senescence, and genome instability (137–140). These processes are intricately involved in cancer and aging.

1.4 Role of Intramolecular DNA G-quadruplex in Telomere Processes

Telomere maintenance involves regulation between “capped” versus “uncapped” states. The “capping” mechanisms used to protect telomere ends involve GQ, POT1, and t-loops, which sequester ssTEL to suppress DNA damage signals and prevent degradation, recombination, and end-to-end fusion. On the other hand, telomeres need to be uncapped during DNA metabolic processes, such as DNA replication, recombination, repair, telomerase-based extension and ALT-dependent elongation, in order to make the ssTEL accessible to involved proteins, including telomerase and WRN and BLM helicases.

An example that illustrates this is a proposed model thought to be involved in regulating ssTEL binding by replication protein A (RPA) and POT1 (141). POT1 is thought to suppress activation of the ataxia telangiectasia and Rad3-related (ATR) dependent DNA damage response (DDR) by competitively inhibiting RPA binding to ssTEL (142, 143), which, in turn, is known to trigger the ATR signaling (144). However, POT1/TPP1 was found to be inefficient at preventing RPA binding to telomeric ssDNA *in vitro* (141), although Ray et al. (2014) suggests that telomeric GQ may enhance this ability (145). Flynn et al. (2011) discovered that hnRNPA1 specifically displaces RPA from ssTEL, but not POT1 (141). This RPA displacing activity is inhibited by the telomeric repeat-containing RNA (TERRA) in the early S phase, but then restarted in late S phase when TERRA levels decline (146). Additionally, TERRA was found to promote POT1 binding to ssTEL by removing hnRNPA1, which suggested that the

reaccumulation of TERRA after S phase helps complete the RPA-to-hnRNPA1-to-POT1 switch on ssTEL to transition from the “uncapped” state to the “capped” state after DNA replication (141). This coordination of events is likely to be one of many mechanisms involved in RPA/POT1 regulation. Takai et al. (2011) proposed that binding of POT1/TPP1 to TIN2 also better enabled POT1 to compete against RPA by increasing the rate of POT1 binding, which then enhances the stability of the POT1/TPP1 complex on ssTEL (147).

The fact that all three of these ssTEL binding proteins, RPA (148), POT1 (127), and hnRNPA1 (149), are able to actively unfold GQ provides strong evidence for its participation in telomere maintenance. Additionally, GQ has been found to form preferentially at the very 3' end of telomeric DNA (150). This is significant because it suggests that GQ is involved in regulating processes that depend on accessibility to the 3' terminus, which includes both telomere length maintenance mechanisms: telomerase-based extension and ALT pathway lengthening. Wang et al. (2011) provided evidence for this by systematically studying the size of the 3' tail required for telomeric GQ unwinding, telomerase-based extension, and ALT pathway lengthening, which they determined to be 6 nucleotides (nt), 8 nt, and 12 nt, respectively (151).

Zahler et al. (1991) was the first to show that GQ folding may directly inhibit telomerase activity (35). This suggested that GQ unfolding by hPOT1 may be a mechanism by which it can enhance telomerase extension (127, 152, 153). Zaug et al. (2005) proposed that hPOT1 disrupts intramolecular telomeric GQ and traps the ssTEL in an unfolded state to make the 3' tail available for telomerase extension (127).

However, more lines of evidence have pointed to POT1 having an inhibitory effect on telomerase activity both *in vitro* (154, 155) and *in vivo* (122, 133, 136). This suggests that POT1 can be both a positive and a negative regulator of telomerase extension, and that its effect may be conditional on where it is bound. Lei et al. (2005) explored this possibility and showed that when hPOT1 is bound at the end of the ssTEL, it blocks access and inhibits telomerase activity (154, 155), but is able to increase the activity and repeat addition processivity of telomerase when bound more internally on the ssTEL, where it can leave the 3' tail accessible (155).

Additionally, the POT1/TPP1 heterodimer was found to enhance this positive effect and significantly increase telomerase processivity (156–160). Latrick & Cech (2010) suggested that POT1/TPP1 increases processivity by slowing primer dissociation when telomerase is actively synthesizing DNA and increasing translocation efficiency (158). In addition, Xin et al. (2007)

reported that the POT1/TPP1 heterodimer also enhances POT1 affinity for ssTEL by 5-10 fold (157), which is consistent with the role of the POT1/TPP1 heterodimer in protecting ssTEL from DNA damage response (DDR) machinery (147). Further evidence supporting this protective role came from Ray et al. (2014), which suggested that telomeric GQ enhances the ability of POT1/TPP1 to prevent RPA binding, an ATR-mediated DDR signal (145).

Hwang et al. (2012) presented a potential mechanism for this by demonstrating that POT1/TPP1 displays sliding behavior on ssTEL, which is distinct from the static GQ unfolding behavior that they saw in POT1 alone (161). This difference in behavior suggests that when POT1 binds to ssTEL alone, its preference to start from the 3' tail and its static GQ unfolding/binding nature renders the 3' tail inaccessible to telomerase. However, when it interacts with TPP1, the POT1/TPP1 heterodimer exhibits this distinct sliding behavior and dynamic GQ folding and unfolding behavior, to make the 3' tail accessible and partially resolved of GQ. This behavior may also explain one means by which POT1/TPP1 may enhance telomerase processivity (156, 157), although it is not likely to be the only means (160).

Furthermore, Paeschke et al. (2005) provided evidence for the cell-cycle dependent regulation of GQ formation by ciliate telomere end-binding proteins, TEBP α and TEBP β , which are orthologs of POT1 and TPP1, respectively (162). They found that while TEBPs actively stabilize GQ for most of the cell cycle, during the S-phase, TEBP β is phosphorylated and dissociated from the TEBP α -ssTEL complex, and causes GQ to be resolved, making the 3' terminus accessible to telomerase. This can be explained by the static GQ unfolding to sliding model proposed by Hwang et al. (2012), where POT1/TPP1 allows dynamic GQ, but when TPP1 dissociates, POT1 switches to its GQ unfolding configuration to stably resolve GQ (161). This suggests that the interaction between TPP1 and POT1 can act as a function switch to for POT1's GQ resolving behavior *in vivo*, and that TPP1 may stimulate telomerase processivity by this mechanism.

In addition to this, studies using small molecule GQ stabilizers revealed that they decrease telomerase efficiency (163) while also inhibiting POT1 binding to telomeres and inducing its dissociation from ssTEL (164–166). These findings point to the interplay between GQ and POT1 in regulating accessibility to the 3' tail, and the dependence of their effects on distance from the 3' terminus.

Telomeric GQ structures may also be involved in regulating the ALT pathway, which requires at least 12 free nucleotides (nt) at the 3' end of the ssTEL to invade the duplex region of telomeric DNA and hybridize with a C-rich strand to initiate template extension (114, 151). A limited tail size and presence of GQ is thought to discourage both invasion and annealing. GQ formation at the very 3' end may also interfere with T-loop formation, which provides protection to the telomere end and is prevalent in ALT cell lines (88).

Additionally, since ALT is mediated by homologous recombination, proteins that are involved in recombination and DNA replication activate this pathway. Of these proteins, the ones that bind to ssTEL from the 3' end include RecQ family helicases, WRN (44, 167) and BLM (59), which are known to have GQ unwinding abilities (118, 130, 168, 169), but require ssDNA of sufficient size to load from the 3' tail (170). Hwang et al. (2014) confirmed that WRN and BLM passively bound to ssTEL in an accessibility dependent manner (171).

Temime-Smaali et al. (2009) showed that binding of Topoisomerase III α (Topo III) to the ssTEL is modulated by GQ formation and that its binding is inhibited by telomestatin, a GQ binding ligand, in ALT cell lines. This disruption to the ALT pathway uncaps telomeres (172). Thus, while telomeric GQ folding normally plays a protective role by telomere capping, its formation during replication of duplex telomeric repeats may adversely affect telomere integrity by causing replication fork arrest and DNA breakage within the telomeric tract, which may lead to telomere fragmentation and loss if left unresolved (162).

The diverse conformations and dynamics of intramolecular telomeric GQs (11–26, 34) may implicate distinct interactions with various proteins and ligands. Kinetic studies showed that human telomeric GQs, in near-physiological conditions, spend minimal time in an unfolded state and has extremely fast folding kinetics (9, 173, 174), with which would affect the nature and kinetics of GQ-protein interactions. Many studies have also reported that antiparallel and parallel telomeric GQ structures can coexist and interconvert under near-physiological conditions (9, 10, 20, 145, 175). In telomeric GQ-protein interactions, anti-parallel intramolecular GQ structures have been found to be resistant to telomerase extension *in vivo* (35, 127, 176), while parallel intermolecular GQ structures allow telomerase extension (176). Ray et al. (2014) determined that POT1 unfolds the majority of antiparallel GQ, while the parallel conformation remains folded (145).

G-quadruplex structures may play an important role in regulating accessibility of the 3' end of telomeres to proteins that are involved in a variety of telomeric processes, including telomere end protection and telomere length maintenance. By capping the 3' tail and making it inaccessible, GQ structures inhibit the binding of proteins that need an open 3' tail to load, such as telomerase and the BLM and WRN helicases, which are involved in telomerase-based elongation and ALT-based lengthening, respectively. This gives an advantage to those proteins that have some capability to actively disrupt and unfold GQ, such as POT1, which typically play an important regulatory role through its dynamic interplay with other telomere-associated proteins, including the passive ssTEL binding proteins.

1.5 Oxidative Stress and its Effect on Telomeres and G-quadruplex Structures

Oxidative DNA damage compromises genome integrity and is the result of reactive oxygen species (ROS), which are naturally formed as a byproduct of the mitochondrial respiratory chain. Although ROS play important physiological roles in healthy cells, it gradually accumulates and causes gradual accumulation of oxidative DNA damage (177). In turn, oxidative DNA damage is thought to accelerate telomere shortening and cellular senescence, which are considered hallmarks of the aging process (178, 179). DNA bases are particularly susceptible to ROS, and resultant base damages may be mutagenic, leading to base mispairing, blockage of DNA polymerase during replication, altered affinity for DNA binding proteins, and genomic instability, if left unrepaired (180).

Telomere shortening and oxidative damage, independently as well as cooperatively, trigger senescence, apoptosis, and genomic instability, which are key events in cancer and aging. Harley et al. (1990) showed that telomere attrition with increasing age is an element in the pathobiology of human diseases, particularly aging associated diseases such as cancer and premature aging syndromes (90). Also, oxidative DNA damage on telomeric DNA compromises telomere integrity and plays a role in accelerating telomere attrition and cellular aging (179, 181–183), and in triggering a persistent DNA damage response (184). Von Zglinicki et al. (1995) demonstrated that hyperoxic stress conditions prevent proliferation and cause an increase in the rate of telomere shortening from 90 bp per population doubling (PD) to 500 bp per PD (185). They also showed that the telomere lengths of these treated cells were as short as those of senescent cells, suggesting that telomere shortening leads to proliferative senescence. Petersen et

al. (1998) showed that free radical-mediated accumulation of telomeric single-stranded breaks (SSBs), under conditions of hyperoxia, is dependent on applied oxidative stress and significantly contributes to an accelerated rate of telomere shortening, which in turn leads to a loss of distal telomere fragments and accelerated aging (186). Conversely, accelerated telomere attrition can be countered with anti-oxidative treatments, such as intracellular vitamin C (179, 187).

Brandl et al. (2011) showed that acute stress conditions cause significantly shortened, telomeres, but that attrition happens gradually with time and not immediately after exposure, suggesting that oxidative damage may be retained in telomeres (188). Harbo et al. (2012) then showed that acute oxidative stress results in an increased number of ultra-short telomeres, even in telomerase positive cells, and that the number of ultra-short telomeres correlates strongly with the percentage of senescent cells, while the mean telomere length does not (181). This suggests that damage inducing ultra-short telomeres lead to senescence, rather than gradual attrition.

Telomeric DNA is particularly susceptible to single-stranded breaks (SSBs) and base damage by oxidation, due to its G-rich nature and inability to repair as efficiently as elsewhere in the chromosome (186, 189). The efficacy of repair on telomeres is affected by structure, with fork-openings, D-loops, and 3' overhang repairing less effectively, and by telomere-associated proteins, such as POT1, which have been shown to hinder access of repair proteins to telomeres and lead to accumulation of abasic sites and SSBs (180, 189, 190). These may contribute to accelerated telomere shortening, which in turn triggers a persistent DNA damage response (DDR) during replicative senescence (138, 140, 184). Up to half of the DNA damage foci and all persistent foci are found at telomeres, regardless of telomerase activity, suggesting that telomeres are favored targets of DDR and are important to the aging process (184).

While hTERT can inhibit replicative senescence it cannot rescue premature senescence induced by DNA damage (191). Despite the ability of telomerase to elongate telomeres, under oxidative stress, cells eventually show a G1/S proliferative arrest similar to senescence. For example, in fetal lung fibroblasts, hTERT-mediated immortalization only occurs under hypoxic conditions (192), suggesting that oxidative stress inhibits the ability of telomeres to form functional capped structures despite adequate telomere length. Hewitt et al. (2012) also showed that an age-dependent increase in frequencies of telomere-associated foci occur regardless of telomere length (184).

On the other hand, Vallabhaneni et al. (2013) found that telomerase deficiency exacerbates telomere shortening in Nth1 deficient mouse cells and base excision repair cooperates with telomerase to maintain telomere integrity (182). This suggests that oxidative DNA damage may be the element preventing telomerase activity and processivity, and that other regulatory mechanisms are at play. Findings by Kovalenko et al. (2010) provide evidence for this by showing that TERT contains mitochondria targeting signals and can respond to oxidative stress by localizing to mitochondria, where they can regulate apoptotic responses to oxidative stress (193).

Oxidative DNA damage is mainly repaired by the base excision repair (BER) pathway, which is initiated by a DNA glycosylase that recognizes and excises specific base damage, and also involves coordinating recruitment of endonucleases, polymerases, and ligase proteins (194, 195). Mammalian cells express five DNA glycosylases with overlapping but distinct specificity for various oxidative DNA base lesions: Ogg1, Nth1, Neil1, Neil2, and Neil3 (194, 196). 8-oxoguanine DNA glycosylase 1 (Ogg1) mostly recognizes oxidized guanine lesions from duplex DNA, while endonuclease III-like protein 1 (Nth1) primarily recognizes oxidized pyrimidines from duplex DNA (194). Zhou et al. (2013) determined that Neil3 and Neil1 DNA glycosylases can remove oxidized bases from ssTEL and GQ structures, and that Neil3 exhibits a strong preference for Tg in telomeric sequences and is the only one that has excision activity on Tg in GQ (196). In addition, they showed that none of the glycosylases has activity on GQ DNA containing 8OG. Rhee et al. (2011) also demonstrated that hOgg1 cannot efficiently excise 8OG near a 3' overhang opening (189).

Guanine has the lowest oxidation potential among nucleic acid bases and consecutive runs of guanine within a sequence (ie. telomeres) further lower the oxidation potential (197). Its major oxidative product, 8-oxo-7,8-dihydroguanine (8OG), is one of the most common oxidative DNA lesions, and accumulates in telomeres during oxidative stress (198). Oikawa et al. (2001) found that guanine residues in telomeres are about five times more sensitive to oxidative stress and UV irradiation, with a higher rate of 8OG accumulation and telomere shortening, than in nontelomeric sequences (197). Wang et al. (2010) demonstrated that Ogg1 deficiency results in the accumulation of oxidative 8OG lesions in telomeres and disrupts telomere integrity (199). Additionally, Opresko et al. (2005) showed that 8OG in telomere inhibits telomerase activity and significantly reduces the binding affinity of TRF1 and TRF2 proteins to the duplex telomere

sequence, leading to disruption of telomere length, maintenance and function (200). Binding was disrupted when intermediates of base excision repair, such as abasic sites or single nucleotide gaps, were presented within the telomeric tract, as well. This is significant as TRF2 is directly involved in regulating telomere length and protecting telomeres, which includes doing so by binding with DNA repair proteins (200). On the other hand, telomeric D-loops containing 8OG have also been shown to be preferred substrates for WRN and BLM helicases and POT1 (201). Although 8OG does not block replication by DNA polymerase, if 8OG is left unrepaired, it becomes highly mutagenic and could alter telomeric sequence (202). This alteration can happen by 8OG pairing with adenine, and leading to GC to TA transversions after two rounds of replication (202). These findings indicate that 8OG compromises telomere integrity and plays a role in telomere shortening and cellular aging.

Studies have also shown that 8OG is more reactive and more prone to form in quadruplex than duplex DNA, both in telomeric DNA and non-telomeric regions (203–205). Salt conditions and position of 8OG substitution are known to affect formation and structural dynamics of intramolecular telomeric GQ (198, 203). Studies have shown that when 8OG is incorporated in the end of telomeric guanine triplet, GQ formation is observed, but when it is incorporated in the middle of the triplet, the GQ is further destabilized and multiple structures are produced (198, 203). Szalai et al. (2002) also showed that 8OG incorporation at 5' position of the triplet inhibits telomerase activity, while one in the middle triplet does not (203). However, it is not clear whether the modulation in telomerase activity is due to the disruption of GQ or the oxidation of G to 8OG. Other types of lesions or mutations have been reported to show similar patterns of destabilization depending on position, even though extent of destabilization is dependent on lesion type (206–209). Therefore, further studies are needed to explore the effect of oxidative stress on telomeric GQ structure and its impact on telomere regulation.

1.6 Single-Molecule Förster Resonance Energy Transfer (smFRET)

Single-molecule Förster Resonance Energy Transfer (smFRET) is a powerful spectroscopic technique that measures the efficiency of non-radiative energy transfer between an excited fluorescent donor molecule and an acceptor molecule. The energy transfer occurs by dipole-dipole interaction, and the energy transfer efficiency is dependent on the distance between the donor and acceptor fluorophores, the spectral overlap between donor emission and acceptor

absorption, and the relative orientation of the donor emission and acceptor absorption dipole moments (210). Greater spectral overlap between donor emission and acceptor absorption maximizes energy transfer, while spectral separation between donor and acceptor emissions minimize donor leakage.

Since it is predominantly dependent on dye-to-dye distance, FRET can be used as a molecular ruler with greatest sensitivity in the 30-80 Å range. However, it also needs to be corrected for differences in quantum yield and detection efficiency between the donor and acceptor. The gamma correction factor (γ) is a ratio of change in acceptor intensity to change in donor intensity upon acceptor photobleaching. As an equation, the FRET efficiency, E , is equal to $I_A/(I_A + \gamma I_D)$, where I_A is the acceptor intensity, I_D is the donor intensity and γ is the gamma correction factor (211). Since FRET efficiency is a ratiometric measure, it is independent of the power of the excitation laser.

An imaging modality used for smFRET is total internal reflection fluorescence (TIRF) microscopy, which allows simultaneous observation of multiple DNA-protein interactions with high spatial and temporal resolution readings per pixel. It uses a wide-field microscope and can be set up in two ways: objective-type (oil immersion) or prism-type (water immersion). In prism-type TIRF microscopy (Figure 1), an inverted microscope is used and the excitation beam is focused through a lens and directed through a prism to hit the sample at a shallow incident angle for total internal reflectance (TIR) (212). TIR at the interface between the quartz slide and aqueous imaging buffer creates an evanescent field of illumination, which is used to excite the fluorophores of the surface-immobilized sample at a 100 to 200 nm penetration depth (212). The energy emission of both the donor and acceptor dyes is collected by a water-immersion objective, sent through a long pass filter to remove scattered light, and split into donor and acceptor emission before being sent to a highly sensitive detector.

FRET overcomes the limitations of ensemble measurements, which require population averaging and cannot resolve subpopulations and their non-synchronous dynamics (210). Since FRET can be used as a molecular ruler, changes in FRET can be used to detect structural changes within biological molecules (e.g., GQ folding) or relative motion between two interacting molecules (e.g., DNA-protein interactions), in real-time. For example, GQ formation and unfolding can be monitored via changes in FRET efficiencies (Figure 2). Previous smFRET experiments have been able to reveal the distribution of behaviors in human telomere GQ folding

conformations and dynamics and show interconversion between two different GQ conformations involves an obligatory transient intermediate (10, 175).

1.7 Study Objective

The guanine-rich nature of human telomeric DNA allows it to adopt a G-quadruplex (GQ) secondary structure and also renders it particularly susceptible to the most common oxidative DNA lesion, 8-oxo-guanine. GQ structures at the 3' single-stranded G-overhang are involved in regulating telomere processes that depend on accessibility of the 3' end, such as telomere length maintenance. Likewise, oxidative stress is known to play an important role in telomere length dysregulation and appears to be a major trigger of senescence, apoptosis, and genomic instability, which are key events in cancer and aging. Despite the multitude of studies that relate oxidative stress to telomere regulation, few have studied the effect of oxidative DNA damage on the structural dynamics of the G-overhang and on telomeric DNA-protein interactions. To my knowledge, no study has yet investigated the effect of oxidative DNA damage on single-stranded telomeric GQ in the context of its regulatory role at the 3' terminus. Understanding how oxidative DNA damage affects GQ dynamics will be instrumental for further elucidating the effect of oxidative stress on the interaction between telomeric DNA and telomere-associated proteins. Here, we examine the effect of 8-oxo-guanine on the structural dynamics of telomeric GQ and investigate the implications it may have for the accessibility of the 3' telomere end.

CHAPTER 2: MATERIALS AND METHODS

2.1 Study Design

We used single molecule FRET to characterize the effect of 8-oxoguanine damage on: 1) the structural dynamics of single-stranded telomeric GQ, 2) accessibility of GQ to passive binding, as modeled by complementary DNA probes, and 3) accessibility of GQ to active binding, as modeled by POT1 binding.

DNA constructs of two different lengths of single-stranded tail were examined: (TTAGGG)₄ with 4 hexameric repeats (G4), which can only form one GQ structure, and (TTAGGG)₈ with 8 hexameric repeats (G8), which has the capability of forming up to two GQ structures. For the oxidative damaged constructs, the 8-oxo-guanine modified base was placed in the 3' most middle G tetrad (8OG-G4, 8OG-G8), where the 8-oxo-G is the most disruptive in GQ folding (198, 203, 206). A mutant control construct with a "C" substitution at the same position was also studied for comparison (G4mut, G8mut). For each construct length, we studied the structural dynamics of the unmodified GQ construct (G4, G8), the 8-oxo-guanine construct (8OG-G4, 8OG-G8), and mutant control construct (G4mut, G8mut).

We studied the passive binding of complementary telomeric probes to model proteins that cannot actively unfold GQ without a 3' tail accessible for loading. These proteins include telomerase and WRN and BLM helicases, which are the key processing enzymes for telomere length maintenance. Hwang et al. (2014) showed that the binding behavior of these proteins was similar to that of the 12 nucleotide (nt) complementary probe (C2); tightly folded GQ DNAs including G4 and G8 yielded the lowest accessibility, whereas G6 and G7 allowed the highest accessibility, likely due to the free single stranded portion of DNA uninvolved in the GQ structure (171). The use of this probe length is in agreement with findings from Wang et al. (2011), which investigated the 3' tail size dependence of telomere extension by telomerase (8 nt minimum), alternative lengthening of telomere (ALT) mechanism (12 nt minimum), and telomere GQ unwinding by helicase (6nt minimum) (151).

For this, we used unlabeled DNA probes with, two (C2) to four (C4) CCCTAA repeats. The longer probe was used to determine if there are any differences in binding efficiency that arise from partial accessibility to DNA substrate or stability of probe binding.

We observed the binding behavior of POT1 as the model for proteins that actively unfold GQ, which include RPA and various hnRNPs.

2.2 DNA Substrates and Preparation

Oligonucleotides, listed in Table 1, were purchased from Integrated DNA Technologies (Coralville, IA) and Midland Certified Reagent (Midland, TX). Unlabeled DNA with a 3' amino-C7 modifier were 3' end-labeled with monofunctional NHS-ester conjugated Cy3 (GE Lifesciences) using ethanol precipitation. Briefly, 10 mM of Cy3 dye was incubated with 0.15 mM of amino modified DNA in 85mM sodium tetraborate buffer (pH 8.5) overnight at room temperature in the dark. The labeled oligonucleotides were purified by ethanol precipitation.

Partial duplex DNA (pdDNA) constructs with an 18 bp long duplex stem and a single-stranded telomeric tail, were used for all experiments, and were prepared by annealing 3'-Cy3 labeled telomere single-stranded DNA (ssDNA) with biotinylated 5'-Cy5 labeled 18mer ssDNA at a molar ratio of 1.5:1 in 10mM Tris-HCl pH 8, 100mM KCl.

2.3 Reaction Conditions

Single molecule FRET experiments were conducted in 20mM Tris-Cl pH 7.5, 100mM KCl. The imaging buffer were supplemented with an oxygen scavenging system (0.8 mg/ml glucose oxidase, 0.8% glucose, 3 mM 6- hydroxy-2,5,7,8-tetramethylchromane-2-carboxylic (Trolox), and 0.03 mg/ml catalase). All buffer materials were purchased from Sigma-Aldrich (St. Louis, MO). All measurements were performed at room temperature (23±1°C).

2.4 Single Molecule FRET Measurements

Single molecule FRET experiments were carried out in flow chambers assembled from PEG passivated quartz slides and coverslips. The quartz slides and coverslips were cleaned by sonication in 2.5% Alconox, acetone, methanol, 1M potassium hydroxide, and torching. They were then coated with a mixture of 97% mPEG-silane (methoxy-PEG5000-silane) and 3% biotin-PEG5000-silane, which were both purchased from Laysan Bio, Inc. (Arab, AL).

A homemade wide-field prism-type total internal reflection fluorescence (TIRF) microscope was used to take measurements. Cy3 donor dyes were excited using a solid-state 532 nm laser. Cy3 and Cy5 emission signals were collected through a water-immersion

objective (Olympus Uplan S-Apo; 100x, NA=1.4) and detected using an electron multiplying charge-coupled device camera (iXon DU-897ECS; Andor Technology). Data were recorded at a time resolution of 100 ms and the imaging frames were processed using custom scripts written in IDL to detect molecules and generate fluorescence intensity time trajectories for each molecule (211).

Biotinylated pdDNA constructs were immobilized to PEG passivated surfaces via biotin-neutravidin interaction, and solutions with substrates, probes, and proteins were flown through chambers using a syringe pump at a rate of 10 μ l/sec. For each assay condition, 30 short movies were taken before flowing in the oligo probes or POT1 protein, and again 15 minutes after, to generate smFRET histograms. A series of long movies were taken before and after flow as well to generate FRET traces. One long movie was taken at the time of flowing in the oligo probes or POT1 protein, to capture flow kinetics. 10 nM of C2-C4 oligo were used for passive probe binding experiments, and 400 nM of POT1 was used for active POT1 binding experiments. Recombinant human POT1 proteins were generously provided by Patricia Opresko (University of Pittsburgh) and purified by Noah Buncher from her lab, using a baculovirus/insect cell expression system described previously (213).

2.5 Data Analysis

Single molecule traces were viewed and analyzed using MATLAB. FRET efficiency, E , was calculated as a ratio between the acceptor intensity and the total donor and acceptor intensity. The values were corrected for background and donor leakage into the acceptor channel. The initial 10 frames of over 7000 smFRET traces were binned into FRET histograms. A threshold was applied based on fluorescence intensities and histograms were normalized.

The peak-to-peak times between dynamic state transitions and the time from flow of probes and POT1 to time of binding (δt), were collected from individual smFRET traces using MATLAB. The individual dwell times for over 200 molecules were binned into dwell-time histograms and fitted to a single exponential decay to calculate the half-life using Origin 9.0 (OriginLab Corporation, Northampton, MA). Binning sizes varied based on the type and range of data collected. Means and standard errors were calculated for all parameters.

CHAPTER 3: RESULTS AND DISCUSSION

3.1 DNA Structural Dynamics

We studied the conformation and structural dynamics of G4 and G8 constructs with and without 8-oxo-guanine modification. The two FRET pair dyes, Cy3 and Cy5, were positioned at either end of the GQ forming DNA and exhibited high FRET when GQ folding occurred. The FRET histogram was built from FRET values collected from over seven thousand DNA molecules imaged on a surface, while the single molecule traces came from a single DNA molecule. The G4 DNA construct displays a steady high FRET state (0.9), indicative of a stable GQ conformation (Figure 3a-c; top). In contrast, both mutant substrates exhibited a distinct and decreased FRET state, revealing a flexible secondary structure. The slightly lower FRET state of 8OG-G4 (Figure 3a-c; bottom) compared to G4mut (Figure 3a-c; middle), suggests that 8OG causes a greater disruption in GQ secondary structure than a base pair substitution. Additionally, G4mut showed occasional transient FRET fluctuations (<2 sec) from 0.75 to 0.84-0.9, while 8OG-G4 showed frequent and highly dynamic transitions from 0.66 to 0.84-0.9. The dynamics to high FRET state suggests that the substrates can still achieve a tight GQ conformation and is inclined to this GQ state despite destabilization. The rate at which these transient events occur (δt) was analyzed for both mutant constructs (Figure 3d). 8OG-G4 was found to have a faster rate of dynamics than G4mut, with a half-life of 3.8 seconds and 17.7 seconds, respectively. Together, these findings provide evidence for greater destabilization in the 8OG model than in the base substitution substrate, although both mutants are destabilized relative to the control construct with tight GQ conformation.

For G8 length constructs, G8 (Figure 4; left) shows a great variety of static and dynamic smtraces with transient dips at various FRET states, and the diversity of populations is evident in its smFRET histogram. G8mut (Figure 4; middle) shows occasional transitions from predominantly 0.48 and 0.59, with the major population at 0.48 and minor population at 0.59. 8OG-G8 (Figure 4; right) reveals an unresolved FRET histogram indicative of a flexible secondary structure, with a peak at 0.49. Single molecule traces also show that 8OG-G8 is predominantly in the loosely folded (one GQ) state with frequent and fast transitions to a tightly folded two GQ state. 8OG-G8 appears to show faster dynamics compared to G8mut as evidenced by a lower percentage of static and stepping traces and significantly higher transiently

dynamic traces. The greater diversity of dynamic behavior seen in G8 and the consistent pattern of transient dynamics seen in G8mut and 8OG-G8 suggest that G8mut and 8OG-G8 constructs may be “closed” by the mutation at the end G-triplet, which restricts their dynamic behavior. Patterns in conformational dynamics between G8mut and 8OG-G8 parallels those seen in the G4 length constructs.

3.2 Probe Accessibility

We determined the accessibility of telomeric ssDNA constructs by passive binding to complementary probes of different lengths. As anticipated, G4 (Figure 5b) was inaccessible by any probe length. G4mut (Figure 5c) and 8OG-G4 (Figure 5d) shifted its FRET states readily for all probe lengths, suggesting that they are fully accessible for all probes. Since up to two probes may bind to G4 length constructs, we were able to see two distinct bound FRET states, 0.55 (1 probe) and 0.3 (2 probes) for G4mut substrates. However, we only saw one FRET state indicating 2 probe binding for 8OG-G4, suggesting that 8OG-G4 is more readily accessible than G4mut.

For G8 length constructs, G8 (Figure 6; left) showed minimal change after addition of C2 and C4 length probes, with partial accessibility for the C3 probe. Interestingly, the partial accessibility seen in G8 seems to occur in the low FRET G8 conformations, which is thought to be representative of one GQ structure and a relaxed conformation in the accessible region, as opposed to tight conformation with two GQ structures as indicated by the high FRET population. G8mut (Figure 6; middle) and 8OG-G8 (Figure 6; right) showed FRET shifts after addition of all probes, indicating accessibility. Furthermore, greater FRET shifts were seen with binding by longer probes. In all, the pattern of accessibility for the G8 length constructs paralleled those of the G4 length constructs.

The % accessibility for each construct and probe condition was calculated by subtracting normalized histograms taken before and after probe binding and dividing that by the normalized histogram before probe binding (Figure 7). Histogram subtraction suggests that mutant constructs have greater (or quicker) accessibility than control constructs. G4 is not accessible by any of the probe lengths, while G8 is minimally accessible, with partial accessibility using the C3 probe. G4mut and 8OG-G4 are fully accessible for all probes, while G8mut and 8OG-G8 are mostly accessible, but with less accessible for the C2 probe. G8mut and 8OG-G8 showed

greater accessibility for C3 and C4, with slightly greater accessibility using C3. These preliminary results suggest G8mut has slightly greater % accessibility than 8OG-G8, but further study is needed due to the complexity of G8 behavior.

For our kinetic analysis on G4 length constructs, we measured the time to probe binding (δt) (Figure 8). 8OG-G4 was found to have faster binding kinetics than G4mut for all probe lengths. Of note, binding of the C4 probe was very slow for the G4mut construct, suggesting G4mut may have a secondary structure with stronger intramolecular bonds that make binding of a probe with the same length as the construct, more difficult. However, C3 probe exhibited the fastest binding for G4mut, with 78% binding, compared to 65% binding for C2 and 50% binding for C4, seen within first two minutes (data not shown). The slower time seen by C2 probe binding may be due to the extra time needed for second probe binding. Additionally, a significant minority group of traces exhibited two step binding for all probes, indicating an intermediate step in one probe binding. Interestingly, it was relatively rare in C2 probe binding and more often seen in C3 and C4 probe binding. The intermediate steps were observed less in the 8OG-G4 substrate. Binding kinetics may be affected, in part, by the intrinsic differences in dynamic patterns between the two mutant constructs before probe binding. As discussed earlier, G4mut displays slower dynamics to tight GQ conformation state than 8OG-G4.

In smtraces, G8 appeared to have more traces that show binding, but it is difficult to resolve because the inherent G8 behavior shows transitions from higher to lower FRET states that cannot be distinguished from probe binding. G8mut showed faster and more effective binding for C3 probes than C4 probes and C2 probes. Additionally, G8 length constructs appeared to bind slower than G4 length constructs, which is as expected due to how many probes can bind. 8OG-G8 appeared to bind faster than G8mut for all constructs. Further analysis was complicated by the complex and highly variable nature of G8 length constructs. Probe binding was difficult to resolve from intrinsic DNA behavior and bound, unbound, and photobleaching/donor only events had overlapping thresholds. Despite these complications, our observations suggest the behavior of G8 length constructs parallel behavior of corresponding G4 length constructs. Also of note, dissociation of probe after binding was not seen.

3.3 POT1 Binding

The G4 control construct does not exhibit immediate binding like G4 length mutant constructs. As expected, G4 showed only partial GQ unfolding in K⁺ conditions due to existence of both antiparallel and parallel GQ conformations (145). Trace analysis for G4 revealed that of the molecule bound, 88% of traces display a stable binding process, mostly from one-step binding from 0.88 to 0.45, while the other 12% display a dynamic binding process, suggestive of POT1 struggling to disrupt GQ before stably binding. Later traces indicated that POT1 remains stably bound. In G4mut, binding happened immediately, with 33% exhibiting dynamic binding processes that extended before stable binding. About 8.5% continued dynamic fluctuations. In 8OG-G4, there were very few dynamic binding processes and most traces showed immediate binding. However, ~12% displayed more erratic dynamics indicative of dynamic interactions or unstable binding with similar dynamic fluctuations in later traces.

For the G8 control construct, ~30% of molecules showed dynamics before and after POT1 binding. 35% stable binding was seen within two minutes and 10-15% occurred later. 22% of traces showed dynamic binding. In G8mut, ~81% bound with about half showing dynamic or unstable binding and 38% showing dynamic binding later. For 8OG-G8, 78% bound with ~39% displaying dynamic or unstable binding within the first two minutes and 24% displaying dynamics later, suggesting that they somewhat appear to stabilize. Dissociation of POT1 was rarely seen. Thus, study of traces showed that a population of base substitution mutants has binding processes, while 8OG mutants show unstable binding.

Calculations of accessibility to POT1 using histogram subtraction for both G4 length constructs and G8 length constructs indicate that base substitution has greater accessibility than 8OG, which in turn has greater accessibility than control construct. For the G4 length constructs (Figure 9), G4mut was found to be 97.5% accessible, while 8OG-G4 was found to be 85.5% and G4 was 52.3%. For the G8 length constructs (Figure 9), G8mut was found to be 84.3% accessible, while 8OG-G8 was 68.8% and G8 was 65.9%. Additionally, study of POT1 binding time, showed that 8OG-G4 bound faster than G4mut, and both were much faster than G4 (Figure 10). The average binding time for G4mut was found to be 7.82 seconds and that of 8OG-G4 was found to be 4.75 seconds. This is similar to an exponential fitting used to determine a half-life of 7.4 seconds for G4mut and a half-life of 4.2 seconds for 8OG-G4. Fitting to a cumulative distribution curve (Figure 11) showed that 8OG-G4 binds faster but then plateaus at a lower % of

bound molecules than G4mut. This is similar to estimates taken by frequency count of smtraces and % accessibility calculated.

Histogram subtraction and frequency counts in smtraces both seem to suggest a slightly lower accessibility for 8OG construct compared to the single base substitution. This may be due to the intrinsically faster dynamics seen. However, this result may be affected by an artifact of the differences in FRET values of the DNA constructs and the broader peaks for the 8OG constructs. Another factor to be taken into consideration is the population of high FRET traces that do not readily bind. Since the percentage of this population is variable between runs and is thought to be influenced by experimental conditions, the weight of this population may serve as an artifact that skews these results as well. Further study is needed to fully address the differences in accessibility between mutant constructs.

3.4 Future Directions

Small molecule GQ binding ligands can be used to regulate telomere maintenance by locking telomeric DNA in a GQ conformation. This GQ stabilization is thought to inhibit telomerase activity and POT1 binding (35, 151, 163, 166, 214–218), prevent GQ unwinding, which is required for the ALT pathway (151, 219), and cause rapid dissociation of telomere capping proteins, TRF1 and POT1 (166), which leads to degradation of the ssTEL and an increase in DNA damage signals at the telomeres (54, 164, 165, 220), and ultimately to apoptosis (165, 221).

The involvement of GQ structures in telomere maintenance makes it an attractive target for cancer therapeutics. However, since GQs are involved in all of these telomeric processes, great care needs to be taken to understand the differential effects of various designs of GQ binding ligands. A study by de Cian et al. (2007) dissected the effect of GQ ligands on telomerase inhibition, and found that although most GQ ligands can inhibit the initiation of telomerase extension, only few molecules can interfere with telomerase processivity (222). This highlights the importance of further studying the mechanism of action of GQ binding ligands, which involves developing a better understanding GQ conformations and dynamics in order to improve drug affinity, specificity, and selectivity for cancer cells over normal cells. For example, for targeting ssTEL, drug design may seek excellent selectivity for single stranded DNA over double stranded DNA (164–166) among other parameters.

The results from our study may have implications for the design of GQ binding ligands. Most standard chemo- and radiation- therapies are based on reactive oxygen species (ROS) induction. Therefore, if GQ binding ligands are to be used as an adjuvant therapy, oxidative stress needs to be taken into consideration during drug design. This requires further studies on the effect of oxidative damage at ssTEL, in the context of its impact on GQ ligand binding affinity due to differences in GQ conformation and dynamics, as well as its effect on protein binding and activity.

CHAPTER 4: CONCLUSION

We used single-molecule FRET to characterize the effect of oxidative stress on the structural dynamics and accessibility of single-stranded human telomeric DNA (ssTEL). Stable and tight G-quadruplex (GQ) folding observed in K⁺ salt conditions was disrupted by a single 8-oxoguanine (8OG) mutation and generated rapid dynamics from looser secondary conformation to a tighter GQ folded state. Although both mutations affected Hoogsteen basepairing and G-quadruplex (GQ) stability, 8-oxoguanine (8OG) affected GQ stability more than a single complementary base substitution. Kinetic analysis also showed a higher frequency of dynamics and faster dynamics with 8OG damage than with a single base substitution.

We also determined that the destabilization of GQ secondary structure allows complementary probe binding, which is representative of passive binding of proteins such as WRN and BLM helicases, and telomerase. Kinetic analysis showed faster probe binding in 8OG mutation than single base substitution. Although both mutants showed a great increase in accessibility, 8OG showed slightly lower accessibility, perhaps due to the intrinsically faster dynamics seen. Thus, structural dynamics induced by the 8OG lesion contributes to increased binding of complementary DNA probes, suggesting enhanced accessibility of 3' ssTEL to passively interacting molecules.

Our findings regarding active GQ unfolding by POT1 showed partial GQ unfolding for stable G4 in K⁺ conditions, as expected due to existence of both antiparallel and parallel GQ conformations. In contrast, both mutants were highly accessible, although our results suggest the single base substitution allows greater accessibility than 8OG damage, while 8OG exhibited faster binding kinetics.

Although distinct in nature in accessibility and kinetics, both single base oxidative damage and single base mutation compromise GQ structure and this destabilization leads to enhanced accessibility of the 3' ssTEL tail. This has implications for passively binding proteins that require a 3' tail to load and for actively GQ unfolding proteins. Our findings provide evidence supporting the significance of the GQ secondary structure in telomere regulation, particularly for telomere length maintenance.

FIGURES AND TABLES

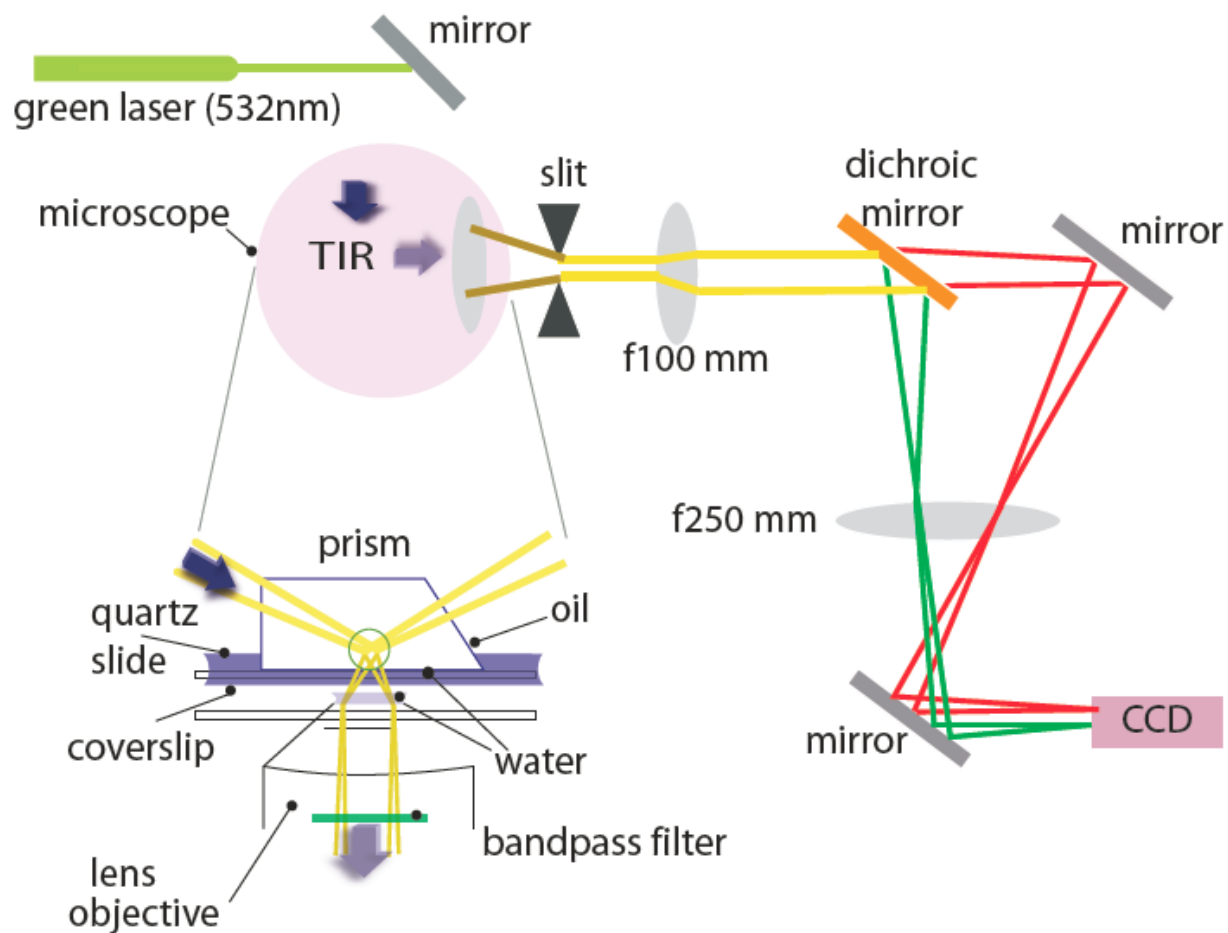


Figure 1. Prism-based total internal reflection fluorescent (TIRF) microscope setup. This imaging modality allows simultaneous observation of multiple single molecule events and interactions for smFRET by high spatial and temporal resolution readings.

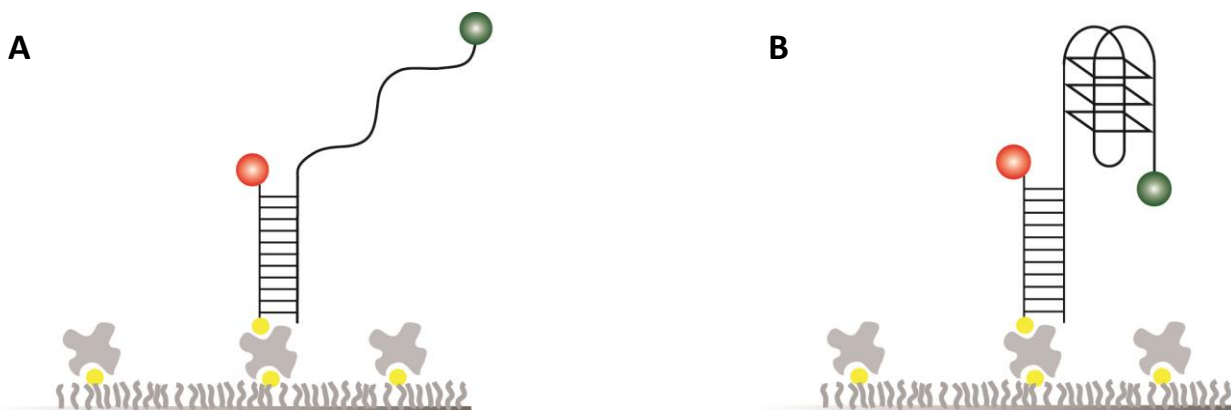


Figure 2. DNA constructs immobilized on PEG-passivated surface via biotin-neutravidin interaction. (A) Construct in a low FRET state suggests an unfolded state, while (B) construct in a high FRET state suggests a folded GQ state.

| Construct | Sequence |
|------------------|--|
| G4 | 5' - TGG CGA CGG CAG CGA GGC TTA GGG TTA GGG TTA GGG TTA GGG /3Cy3/ |
| G8 | 5' - TGG CGA CGG CAG CGA GGC (TTA GGG) ₈ /3Cy3/ |
| G4mut | 5' - TGG CGA CGG CAG CGA GGC TTA GGG TTA GGG TTA GGG TTA GCG /3Cy3/ |
| G8mut | 5' - TGG CGA CGG CAG CGA GGC (TTA GGG) ₇ TTA GCG /3Cy3/ |
| 8-oxo-G4 | 5' - TGG CGA CGG CAG CGA GGC TTA GGG TTA GGG TTA GGG TTA G(8oxodG)G /3Cy3/ |
| 8-oxo-G8 | 5' - TGG CGA CGG CAG CGA GGC (TTA GGG) ₇ TTA G(8oxodG)G /3Cy3/ |
| | |
| 18mer bottom | 5' - /Cy5/ GCC TCG CTG CCG TCG CCA – 3' biotin (annealed to all Cy3 sequences) |
| | |
| Probe | Sequence |
| C2 | 5' - CCC TAA CCC TAA |
| C3 | 5' - CCC TAA CCC TAA CCC TAA |
| C4 | 5' - CCC TAA CCC TAA CCC TAA CCC TAA |

Table 1. DNA Constructs and Probes. The table lists the sequences for the telomeric DNA constructs used at the top, followed by the sequence for the biotinylated 18mer construct annealed to the telomeric DNA constructs. At the bottom are the sequences of the probes used in the passive binding accessibility assay.

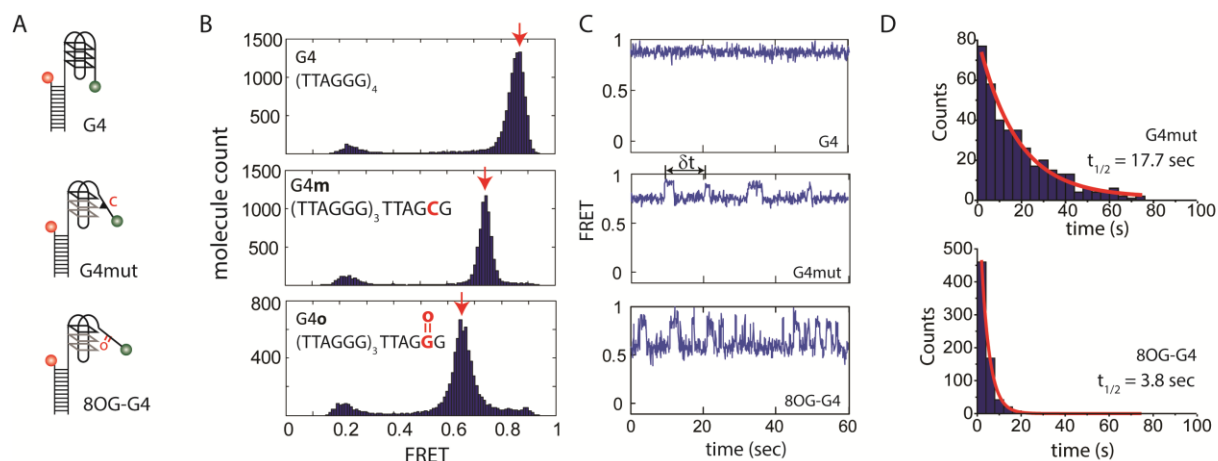


Figure 3. Effect of 8OG on conformation and dynamics of G4 length telomeric overhang. (A) DNA schematics of the three types of constructs: control (G4), complementary single base substitution (G4mut/G4m), and 8-oxo-guanine mutant (8OG-G4/G4o). (B) Single-molecule frequency histograms of DNA show shift in FRET state, indicative of looser secondary structure. (C) Single molecule traces also suggest destabilization as indicated by the transient dynamics to the high FRET “tight” state. (D) Dwell time distribution on mutant constructs confirmed that G4mut has slower rate of dynamics than 8OG-G4, and is fitted with an exponential decay function. The control construct (G4) predominantly remains stable at a very high FRET state (0.9), which suggests a tight GQ conformation.

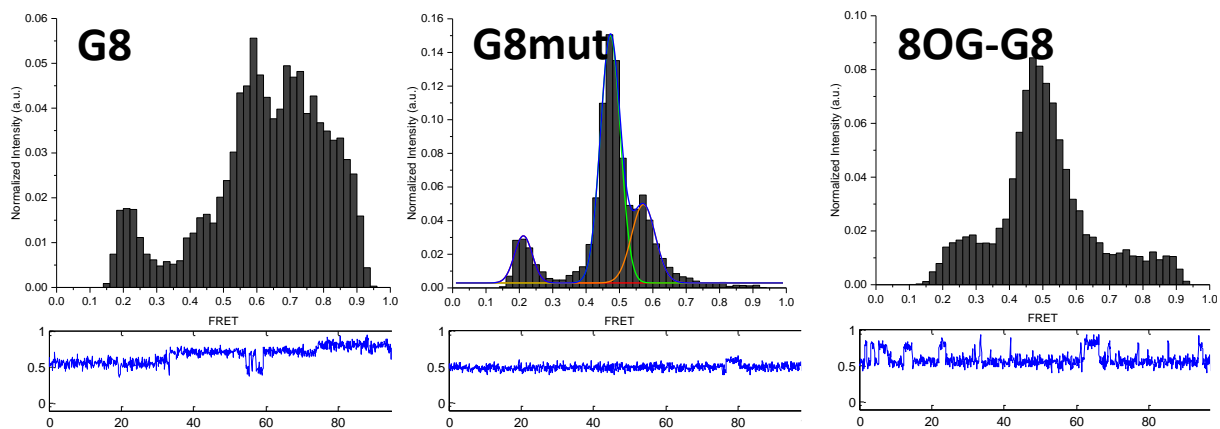


Figure 4. Effect of 8OG on conformation and dynamics of G8 length telomeric overhang. Normalized histogram and representative single molecule trace for G8 (left), G8mut (middle), and 8OG-G8 (right). G8 shows multiple populations of FRET values and the greatest diversity of traces with no predominant pattern. G8mut shows two distinct populations, well fitted with two Gaussian fits, and less frequent and slower dynamics than 8OG-G8, which is less resolved, but typically shows fast dynamics between tightly folded (two GQs) and loosely folded (one GQ) states. This agrees with our observations in the G4 length constructs.

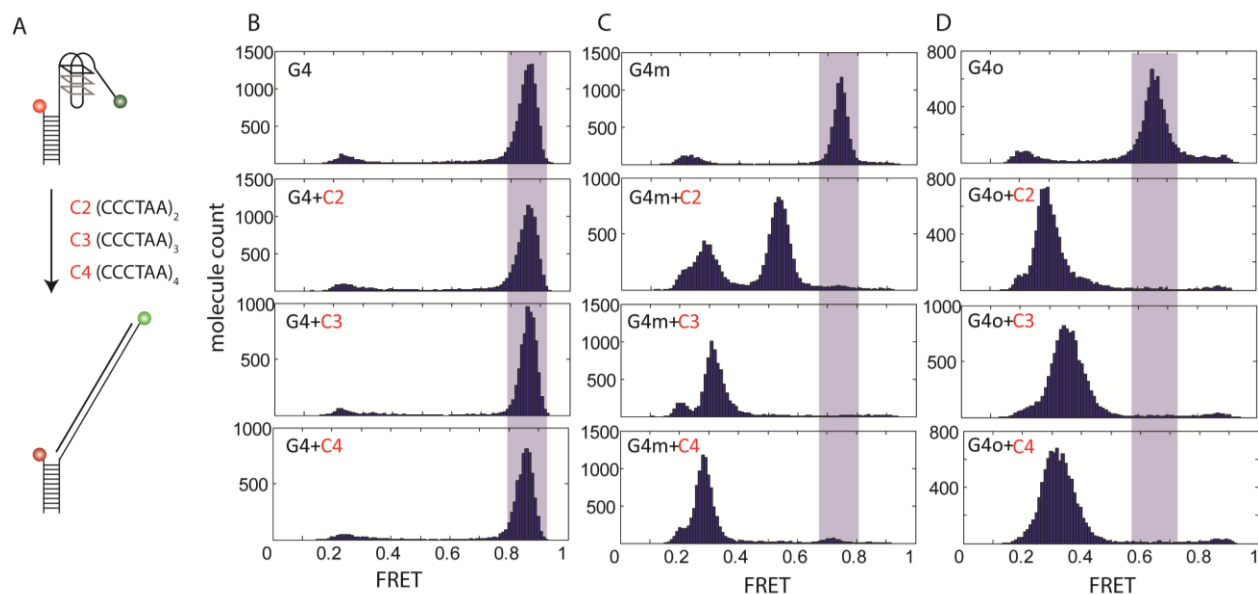


Figure 5. Accessibility of G4 length constructs by C2, C3, and C4. (A) Schematic of how complementary probes may bind to the G4 length constructs. Histograms show before (top row) and after probe binding to illustrate FRET shifts. The blue area indicates the FRET state of construct before probe binding for the G4 (B), G4mut (C), and 8OG-G4 (D) constructs. As can be seen, G4 shows no change and is not accessible by any probe length (C2, C3, C4), while both G4mut and 8OG-G4 shift FRET states readily for all probe lengths. Note that up to two C2 probes may bind to the G4 length constructs, which can be seen in the case of the G4mut construct, which shows two distinct bound FRET states (0.55 and 0.3), indicating one or two probe binding, respectively.

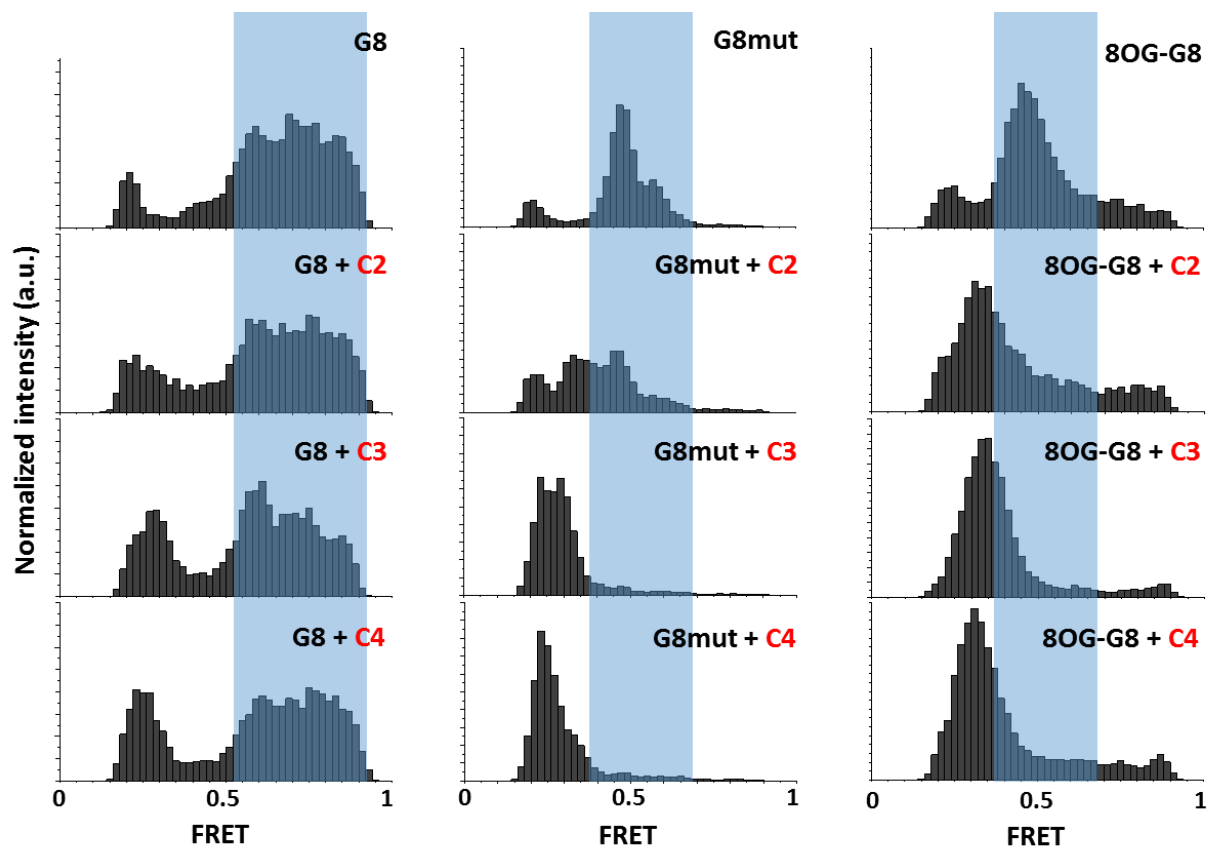
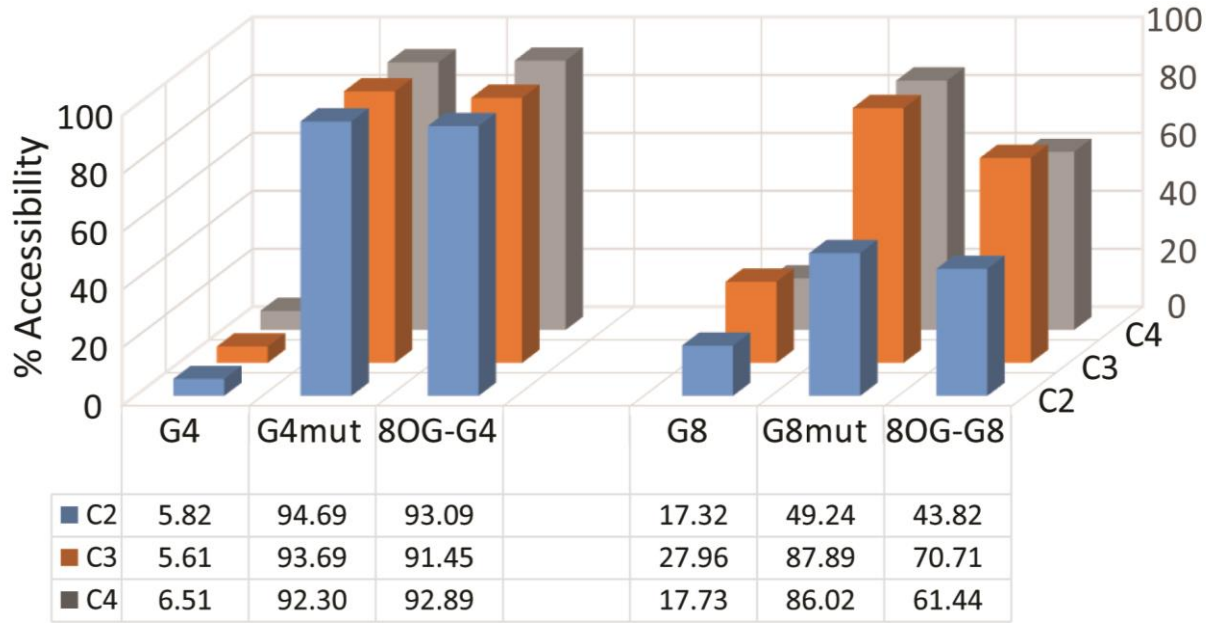


Figure 6. Accessibility of G8 length constructs by C2, C3, and C4. Normalized histogram of G8 (left) construct before (top) and after probe binding shows that G8 has minimal accessibility for the C2 and C4 probe, but partial accessibility with the C3 probe. Meanwhile, G8mut (middle) and 8OG-G8 (right) show greater accessibility: high accessibility for C3 and C4, and partial accessibility for C2. The blue area indicates the FRET state of construct before probe binding.



$$\% \text{ accessibility}_{DNA} = \frac{\left| \sum_{\Delta < 0} FRET_{(DNA+C2)} - FRET_{DNA} \right|}{\sum_{\Delta < 0} FRET_{DNA}} \times 100\%,$$

$$\text{where } \Delta = FRET_{(DNA+C2)} - FRET_{DNA}$$

Figure 7. C2-C4 Accessibility by DNA construct. The % accessibility for each construct and probe condition was calculated by subtracting normalized histograms taken before and after probe binding using the formula provided.

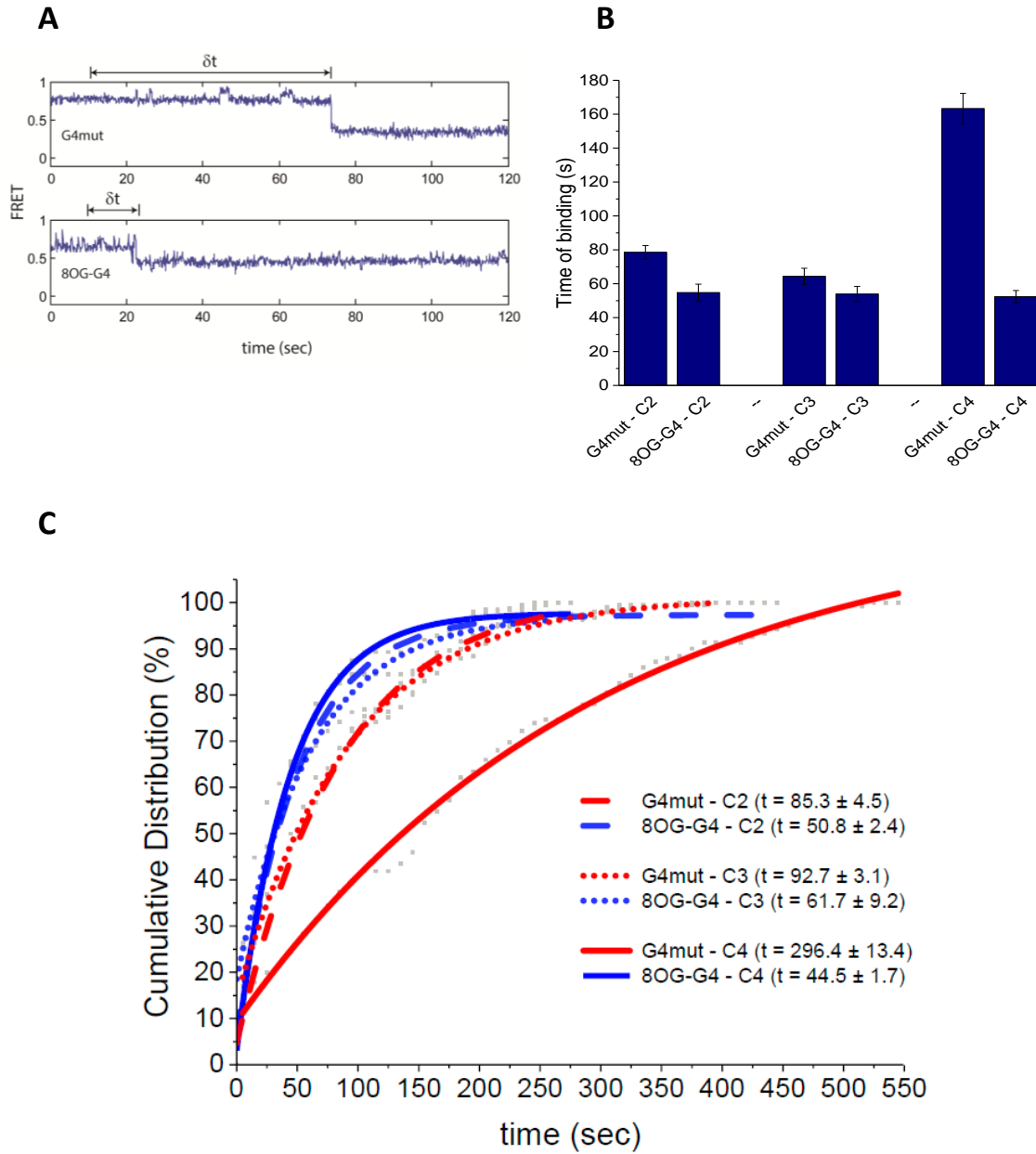


Figure 8. Kinetics of probe binding for G4 length mutant constructs. (A) Single molecule traces were used to measure the time to probe binding (δt). (B) Average binding time was plotted with error bar indicating standard error. (C) Cumulative distribution curve shows the average and was fitted using an exponential growth function. This shows that 8OG-G4 has faster binding kinetics than G4mut for all probe lengths.

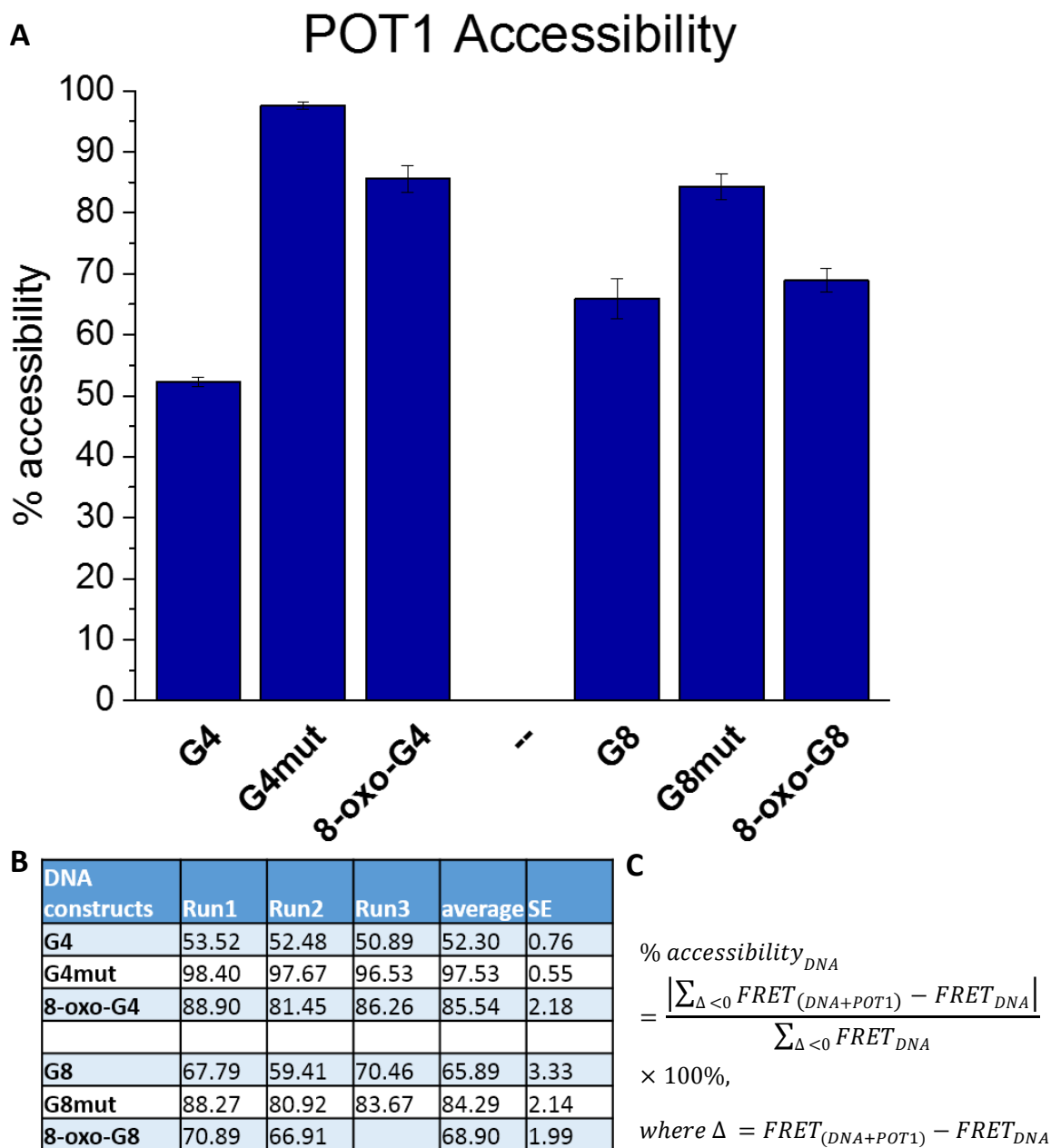


Figure 9. POT1 accessibility by construct. (A) Graph based on average and standard error of 3 separate runs. (B) Table showing % accessibility for each run and values for the average and standard error. (C) Equation used to calculate POT1 accessibility. Results indicate that single base substitution mutant has greater accessibility than 8OG, which in turn has greater accessibility than control construct.

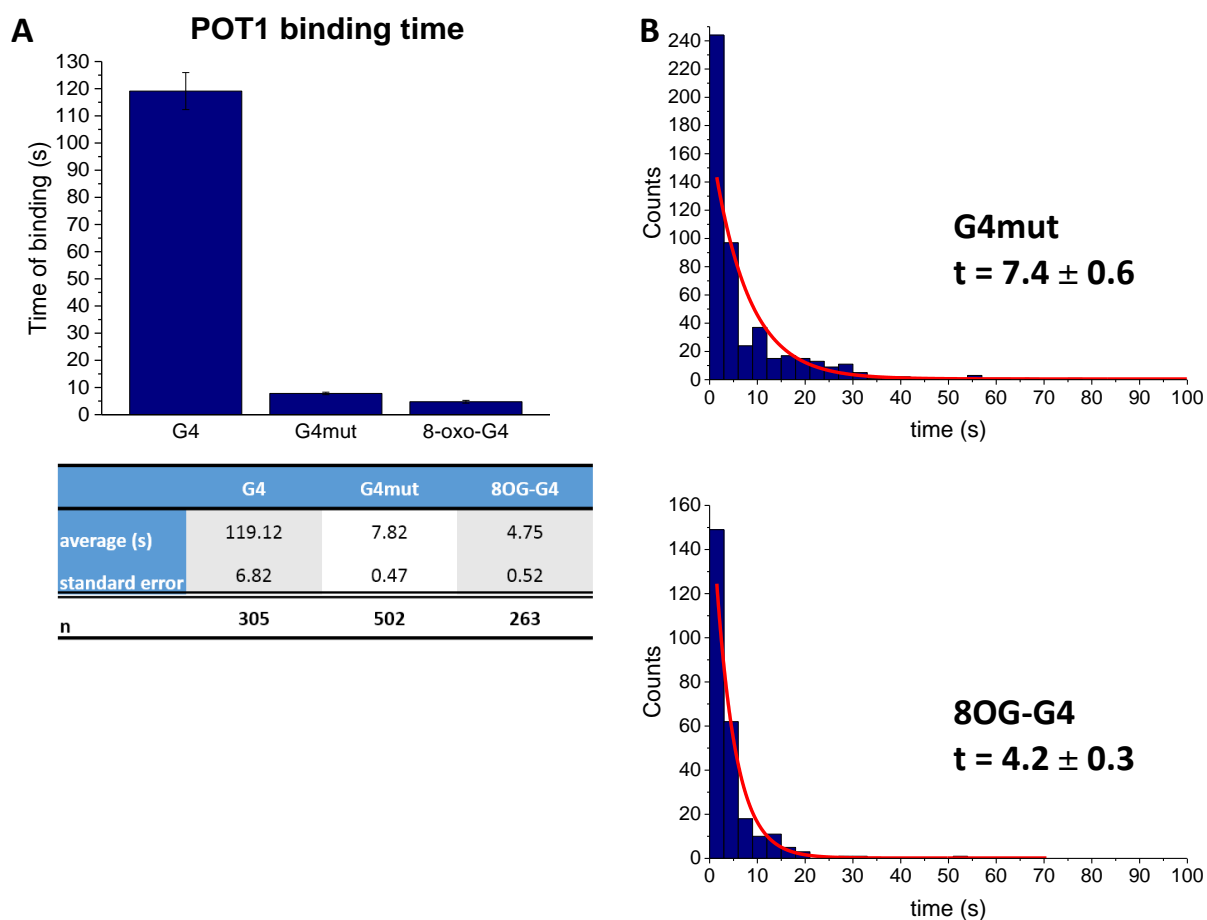


Figure 10. POT1 binding time for G4 length constructs. (A) Graph of POT1 binding time based on average and standard error of data points of n counts as indicated by table below. (B) Dwell time distribution fitted with exponential decay function of POT1 binding time and half-life based on calculations for G4mut (top) and 8OG-G4 (bottom). Findings show that 8OG-G4 binds faster than G4mut, and that both are much faster than G4.

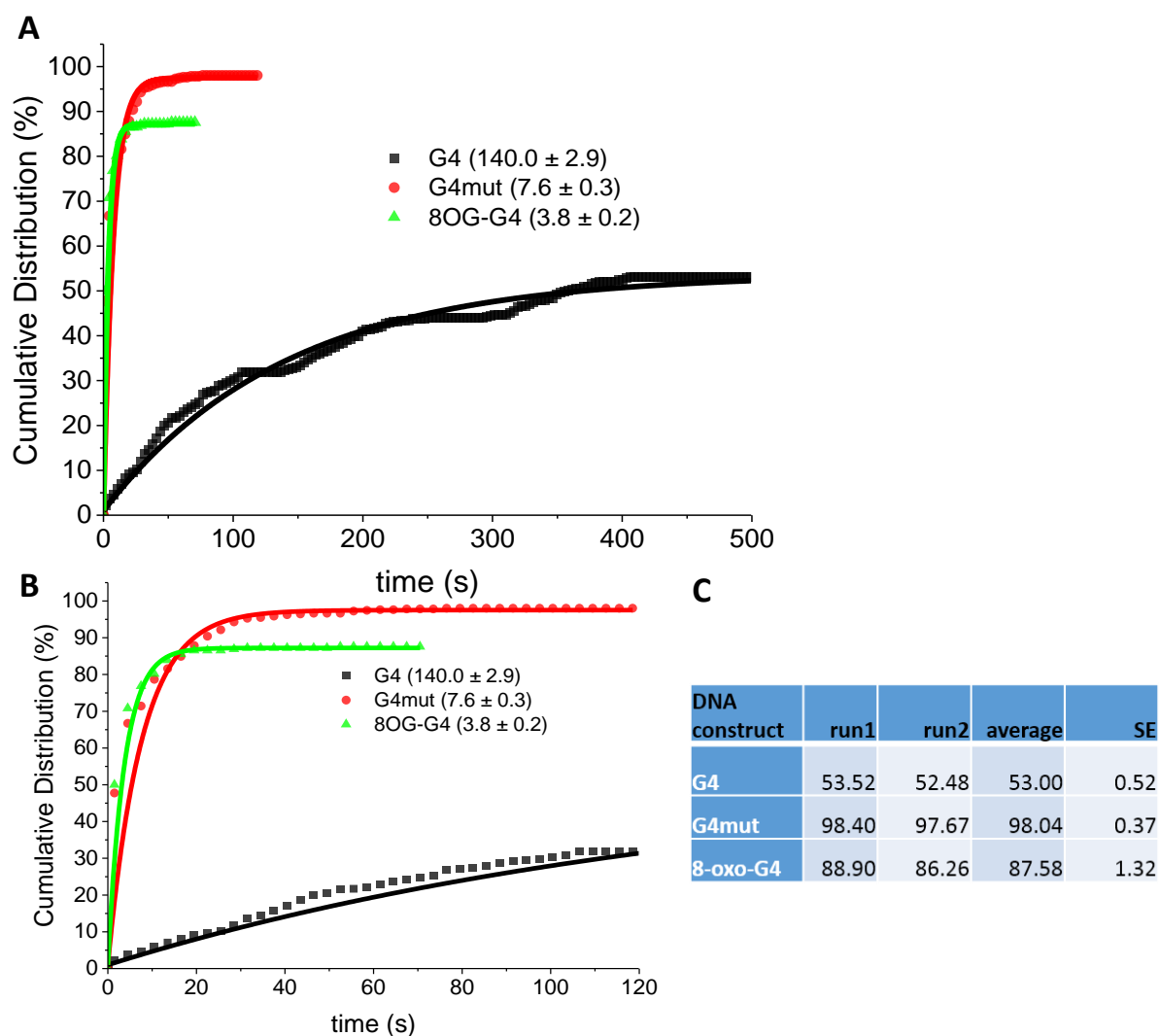


Figure 11. Cumulative distribution curve of POT1 binding time. (A) Cumulative distribution curve was adjusted for % of bound molecules using the average % accessibility calculated. (B) Inset of the cumulative distribution curve showing the first two minutes of POT1 binding. (C) Table of % accessibility for experiments from which data points for dwell time were taken. These results indicate that 8OG-G4 binds faster than G4mut, but plateaus at a smaller % of bound molecules than G4mut.

REFERENCES

1. Gellert M, Lipsett MN, Davies DR (1962) Helix Formation By Guanylic Acid. *Proc Natl Acad Sci* 48(12):2013–2018.
2. Pinnavaia TJ, Marshall CL, Mettler CM (1978) Alkali metal ion specificity in the solution ordering of a nucleotide, 5'-guanosine monophosphate. *J Am Chem Soc* 100:3625–3627.
3. Miles HT, Frazier J (1978) Poly(I) helix formation, dependence on size-specific complexing to alkali metal ions. *J Am Chem Soc* 100:8037–8038.
4. Sen D, Gilbert W (1988) Formation of parallel four-stranded complexes by guanine-rich motifs in DNA and its implications for meiosis. *Nature* 334(28):364–346.
5. Hardin C, Perry A, White K (2001) Thermodynamic and kinetic characterization of the dissociation and assembly of quadruplex nucleic acids. *Biopolymers* 56(3):147–194.
6. Kumar N, Sahoo B, Varun K, Maiti S, Maiti S (2008) Effect of loop length variation on quadruplex-Watson Crick duplex competition. *Nucleic Acids Res* 36(13):4433–42.
7. Keniry MA (2001) Quadruplex structures in nucleic acids. *Biopolymers* 56:123–146.
8. Sen D, Gilbert W (1992) Guanine Quartet Structures. *Methods Enzymol* 211:191–199.
9. Tippana R, Xiao W, Myong S (2014) G-quadruplex conformation and dynamics are determined by loop length and sequence. *Nucleic Acids Res* 42(4):1–9.
10. Lee JY, Okumus B, Kim DS, Ha T (2005) Extreme conformational diversity in human telomeric DNA. *Proc Natl Acad Sci U S A* 102(52):18938–18943.
11. Dai J, Carver M, Yang D (2008) Polymorphism of human telomeric quadruplex structures. *Biochimie* 90(8):1172–83.
12. Gray RD, Trent JO, Chaires JB (2014) Folding and Unfolding Pathways of the Human Telomeric G-Quadruplex. *J Mol Biol.*
13. Dhakal S, et al. (2013) Structural and mechanical properties of individual human telomeric G-quadruplexes in molecularly crowded solutions. *Nucleic Acids Res* 41(6):3915–23.
14. Heddi B, Phan AT (2011) Structure of human telomeric DNA in crowded solution. *J Am Chem Soc* 133(25):9824–33.
15. Lane AN, Chaires JB, Gray RD, Trent JO (2008) Stability and kinetics of G-quadruplex structures. *Nucleic Acids Res* 36(17):5482–515.

16. Xu Y (2011) Chemistry in human telomere biology: structure, function and targeting of telomere DNA/RNA. *Chem Soc Rev* 40(5):2719–40.
17. Burge S, Parkinson GN, Hazel P, Todd AK, Neidle S (2006) Quadruplex DNA: sequence, topology and structure. *Nucleic Acids Res* 34(19):5402–15.
18. Wang Y, Patel DI (1993) Solution structure of the human telomeric repeat d[AG3(T2AG3)3] G-tetraplex. *Curr Biol* 1:263–282.
19. Parkinson GN, Lee MPH, Neidle S (2002) Crystal structure of parallel quadruplexes from human telomeric DNA. *Nature* 417(6891):876–80.
20. Ambrus A, et al. (2006) Human telomeric sequence forms a hybrid-type intramolecular G-quadruplex structure with mixed parallel/antiparallel strands in potassium solution. *Nucleic Acids Res* 34(9):2723–35.
21. Luu KN, Phan AT, Kuryavyi V, Lacroix L, Patel DJ (2006) Structure of the Human Telomere in K⁺ Solution: An Intramolecular (3 + 1) G-Quadruplex Scaffold. *J Am Chem Soc* 129(6):9963–70.
22. Phan AT, Kuryavyi V, Luu KN, Patel DJ (2007) Structure of two intramolecular G-quadruplexes formed by natural human telomere sequences in K⁺ solution. *Nucleic Acids Res* 35(19):6517–25.
23. Dai J, Carver M, Punchihewa C, Jones R a, Yang D (2007) Structure of the Hybrid-2 type intramolecular human telomeric G-quadruplex in K⁺ solution: insights into structure polymorphism of the human telomeric sequence. *Nucleic Acids Res* 35(15):4927–40.
24. Xu Y, Ishizuka T, Kurabayashi K, Komiyama M (2009) Consecutive formation of G-quadruplexes in human telomeric-overhang DNA: a protective capping structure for telomere ends. *Angew Chem Int Ed Engl* 48(42):7833–6.
25. Singh V, Azarkh M, Drescher M, Hartig JS (2012) Conformations of individual quadruplex units studied in the context of extended human telomeric DNA. *Chem Commun* 48(66):8258–60.
26. Hansel R, Lohr F, Trantirek L, Dotsch V (2013) High-Resolution Insight into G-Overhang Architecture. *J Am Chem Soc* 135:2816–2824.
27. Todd AK, Johnston M, Neidle S (2005) Highly prevalent putative quadruplex sequence motifs in human DNA. *Nucleic Acids Res* 33(9):2901–7.
28. Huppert JL, Balasubramanian S (2005) Prevalence of quadruplexes in the human genome. *Nucleic Acids Res* 33(9):2908–16.

29. Huppert JL, Balasubramanian S (2007) G-quadruplexes in promoters throughout the human genome. *Nucleic Acids Res* 35(2):406–413.
30. Eddy J, Maizels N (2006) Gene function correlates with potential for G4 DNA formation in the human genome. *Nucleic Acids Res* 34(14):3887–96.
31. Williamson JR, Raghuraman MK, Cech TR (1989) Monovalent cation-induced structure of telomeric DNA: The G-Quartet Model. *Cell* 59:871–880.
32. Henderson E, Hardin CC, Walk SK, Tinoco Jr I, Blackburn EH (1987) Telomeric DNA oligonucleotides form novel intramolecular structures containing guanine-guanine base pairs. *Cell* 51:899–908.
33. Sundquist WI, Klug A (1989) Telomeric DNA dimerizes by formation of guanine tetrads between hairpin loops. *Nature* 342:825–829.
34. Phan AT, Luu KN, Patel DJ (2006) Different loop arrangements of intramolecular human telomeric (3+1) G-quadruplexes in K⁺ solution. *Nucleic Acids Res* 34(19):5715–9.
35. Zahler AM, Williamson JR, Cech TR, Prescott DM (1991) Inhibition of telomerase by G-quartet DNA structures. *Nature* 350:718–720.
36. Ruden M, Puri N (2013) Novel anticancer therapeutics targeting telomerase. *Cancer Treat Rev* 39(5):444–56.
37. Hammond-kosack MCU, Dobrinski B, Lurz R, Docherty K, Kilpatrick MW (1992) The human insulin gene linked polymorphic region exhibits an altered DNA structure. *Nucleic Acids Res* 20(2):231–236.
38. Murchie AIH, Lilley DMJ (1992) Retinoblastoma susceptibility genes contain 5' sequences with a high propensity to form guanine-tetrad structures. *Nucleic Acids Res* 20(1):49–53.
39. Simonsson T, Pecinka P, Kubista M (1998) DNA tetraplex formation in the control region of c-myc. *Nucleic Acids Res* 26(5):1167–1172.
40. Simonsson T, Sjoback R (1999) DNA Tetraplex Formation Studied with Fluorescence Resonance Energy Transfer. *J Biol Chem* 274(24):17379–17383.
41. Siddiqui-Jain A, Grand CL, Bearss DJ, Hurley LH (2002) Direct evidence for a G-quadruplex in a promoter region and its targeting with a small molecule to repress c-MYC transcription. *Proc Natl Acad Sci U S A* 99(18):11593–8.
42. Bochman ML, Paeschke K, Zakian V a (2012) DNA secondary structures: stability and function of G-quadruplex structures. *Nat Rev Genet* 13(11):770–80.

43. Fernando H, et al. (2009) Genome-wide analysis of a G-quadruplex-specific single-chain antibody that regulates gene expression. *Nucleic Acids Res* 37(20):6716–22.
44. Johnson JE, Cao K, Ryvkin P, Wang L-S, Johnson FB (2010) Altered gene expression in the Werner and Bloom syndromes is associated with sequences having G-quadruplex forming potential. *Nucleic Acids Res* 38(4):1114–22.
45. Larson ED, Duquette ML, Cummings WJ, Streiff RJ, Maizels N (2005) MutSa binds to and promotes synapsis of transcriptionally activated immunoglobulin switch regions. *Curr Biol* 15:470–474.
46. Cahoon L a, Seifert HS (2009) An alternative DNA structure is necessary for pilin antigenic variation in *Neisseria gonorrhoeae*. *Science* 325(5941):764–7.
47. Cahoon L a, Seifert HS (2013) Transcription of a cis-acting, noncoding, small RNA is required for pilin antigenic variation in *Neisseria gonorrhoeae*. *PLoS Pathog* 9(1):e1003074.
48. Nagaraju G, Scully R (2007) Minding the gap: the underground functions of BRCA1 and BRCA2 at stalled replication forks. *DNA Repair (Amst)* 6(7):1018–31.
49. Ribeyre C, et al. (2009) The yeast Pif1 helicase prevents genomic instability caused by G-quadruplex-forming CEB1 sequences in vivo. *PLoS Genet* 5(5):e1000475.
50. Lopes J, et al. (2011) G-quadruplex-induced instability during leading-strand replication. *EMBO J* 30(19):4033–46.
51. Hershman SG, et al. (2008) Genomic distribution and functional analyses of potential G-quadruplex-forming sequences in *Saccharomyces cerevisiae*. *Nucleic Acids Res* 36(1):144–56.
52. Verma A, Yadav VK, Basundra R, Kumar A, Chowdhury S (2009) Evidence of genome-wide G4 DNA-mediated gene expression in human cancer cells. *Nucleic Acids Res* 37(13):4194–204.
53. Wu Y, Shin-ya K, Brosh RM (2008) FANCI helicase defective in Fanconi anemia and breast cancer unwinds G-quadruplex DNA to defend genomic stability. *Mol Cell Biol* 28(12):4116–28.
54. Rodriguez R, et al. (2012) Small molecule-induced DNA damage identifies alternative DNA structures in human genes. *Nat Chem Biol* 8(3):301–310.
55. Huber MD, Lee DC, Maizels N (2002) G4 DNA unwinding by BLM and Sgs1p : substrate specificity and substrate-specific inhibition. *Nucleic Acids Res* 30(18):3954–61.

56. Paeschke K, Capra JA, Zakian VA (2011) DNA replication through G-quadruplex motifs is promoted by the *S. cerevisiae* Pif1 DNA helicase. *Cell* 145(5):678–691.
57. Paeschke K, et al. (2013) Pif1 family helicases suppress genome instability at G-quadruplex motifs. *Nature* 497(7450):458–62.
58. Mohaghegh P, Karow JK, Jr RMB, Bohr VA, Hickson ID (2001) The Bloom's and Werner's syndrome proteins are DNA structure-specific helicases. *Nucleic Acids Res* 29(13):2843–2849.
59. Sun H, Karow JK, Hickson ID, Maizels N (1998) The Bloom's Syndrome Helicase Unwinds G4 DNA. *J Biol Chem* 273(42):27587–27592.
60. Sun H, Yabuki A, Maizels N (2001) A human nuclease specific for G4 DNA. *Proc Natl Acad Sci* 98(22):12444–9.
61. London TBC, et al. (2008) FANCI is a structure-specific DNA helicase associated with the maintenance of genomic G/C tracts. *J Biol Chem* 283(52):36132–9.
62. Cheung I, Schertzer M, Rose A, Lansdorp PM (2002) Disruption of dog-1 in *Caenorhabditis elegans* triggers deletions upstream of guanine-rich DNA. *Nat Genet* 31(4):405–9.
63. Kruisselbrink E, et al. (2008) Mutagenic capacity of endogenous G4 DNA underlies genome instability in FANCI-defective *C. elegans*. *Curr Biol* 18(12):900–5.
64. Koole W, et al. (2014) A Polymerase Theta-dependent repair pathway suppresses extensive genomic instability at endogenous G4 DNA sites. *Nat Commun* 5:3216.
65. Whitehouse I, Smith DJ (2013) Chromatin dynamics at the replication fork: there's more to life than histones. *Curr Opin Genet Dev* 23(2):140–6.
66. Sarkies P, Reams C, Simpson LJ, Sale JE (2010) Epigenetic instability due to defective replication of structured DNA. *Mol Cell* 40(5):703–13.
67. Schwab R a, Nieminuszczy J, Shin-ya K, Niedzwiedz W (2013) FANCI couples replication past natural fork barriers with maintenance of chromatin structure. *J Cell Biol* 201(1):33–48.
68. Sarkies P, et al. (2012) FANCI coordinates two pathways that maintain epigenetic stability at G-quadruplex DNA. *Nucleic Acids Res* 40(4):1485–98.
69. Schaffitzel C, et al. (2001) In vitro generated antibodies specific for telomeric guanine-quadruplex DNA react with *Stylonychia lemnae* macronuclei. *Proc Natl Acad Sci* 98(15):8572–7.

70. Duquette ML, Handa P, Vincent J a, Taylor AF, Maizels N (2004) Intracellular transcription of G-rich DNAs induces formation of G-loops, novel structures containing G4 DNA. *Genes Dev* 18(13):1618–29.
71. Müller S, Kumari S, Rodriguez R, Balasubramanian S (2010) Small-molecule-mediated G-quadruplex isolation from human cells. *Nat Chem* 2(12):1095–1098.
72. Henderson A, et al. (2013) Detection of G-quadruplex DNA in mammalian cells. *Nucleic Acids Res*:1–10.
73. Lam EYN, Beraldi D, Tannahill D, Balasubramanian S (2013) G-quadruplex structures are stable and detectable in human genomic DNA. *Nat Commun* 4:1796.
74. Biffi G, Tannahill D, McCafferty J, Balasubramanian S (2013) Quantitative Visualization of DNA G-quadruplex Structures in Human Cells. *Nat Chem* 5(3):182–186.
75. Greider CW (1996) Telomere length regulation. *Annu Rev Biochem* 65:337–65.
76. Blackburn EH (2001) Switching and signaling at the telomere. *Cell* 106(6):661–73.
77. Sandell LL, Zakian VA (1993) Loss of a yeast telomere: Arrest, recovery, and chromosome loss. *Cell* 75:729–739.
78. Blackburn EH (1991) Structure and function of telomeres. *Nature* 350:569–573.
79. Blackburn EH, Gall JG (1978) A tandemly repeated sequence at the termini of the extrachromosomal ribosomal RNA genes in Tetrahymena. *J Mol Biol* 120:33–53.
80. Oka Y, Shiota S, Nakai S, Nishida Y, Okubo S (1980) Inverted terminal repeat sequence in the macronuclear DNA of Stylonichia pustulata. *Gene* 10:301–306.
81. Klobutcher LA, Swanton MT, Donini P, Prescott DM (1981) All gene-sized DNA molecules in four species of hypotrichs have the same terminal sequence and an unusual 3' terminus. *Proc Natl Acad Sci* 78(5):3015–9.
82. Pluta AF, Kaine BP, Spear BB (1982) The terminal organization of macronuclear DNA in Oxytricha fallax. *Nucleic Acids Res* 10(24):8145–54.
83. Moyzis RK, et al. (1988) A highly conserved repetitive DNA sequence, (TTAGGG)_n, present at the telomeres of human chromosomes. *Proc Natl Acad Sci* 85(September):6622–6626.
84. Zakian VA (1995) Telomeres: beginning to understand the end. *Science* (80-) 270(5242):1601–7.

85. McElligott R, Wellinger RJ (1997) The terminal DNA structure of mammalian chromosomes. *EMBO J* 16(12):3705–14.
86. Wright WE, Tesmer VM, Huffman KE, Levene SD, Shay JW (1997) Normal human chromosomes have long G-rich telomeric overhangs at one end. *Genes Dev* 11(21):2801–2809.
87. De Lange T (2002) Protection of mammalian telomeres. *Oncogene* 21:532–540.
88. Griffith JD, et al. (1999) Mammalian telomeres end in a large duplex loop. *Cell* 97(4):503–14.
89. Xu Y, Sato H, Sannohe Y, Shinohara K, Sugiyama H (2008) Stable lariat formation based on a G-quadruplex scaffold. *J Am Chem Soc* 130(49):16470–1.
90. Harley CB, Futcher AB, Greider CW (1990) Telomeres shorten during ageing of human fibroblasts. *Nature* 345:458–460.
91. Shay JW, Wright WE (2011) Roles of telomeres and telomerase in cancer. *Semin Cancer Biol* 21(6):349–353.
92. Greider CW, Blackburn EH (1985) Identification of a specific telomere terminal transferase activity in Tetrahymena extracts. *Cell* 43(December):405–413.
93. Greider CW, Blackburn EH (1987) The telomere terminal transferase of Tetrahymena is a ribonucleoprotein enzyme with two kinds of primer specificity. *Cell* 51(6):887–98.
94. Greider CW, Blackburn EH (1989) A telomeric sequence in the RNA of Tetrahymena telomerase required for telomere repeat synthesis. *Nature* 337:331–337.
95. Hayflick L, Moorhead PS (1961) The serial cultivation of human diploid cell strains. *Exp Cell Res* 25(3):585–621.
96. Allsopp RC, et al. (1992) Telomere length predicts replicative capacity of human fibroblasts. *Proc Natl Acad Sci* 89(21):10114–8.
97. Maser RS, DePinho R a (2002) Connecting chromosomes, crisis, and cancer. *Science* 297(5581):565–9.
98. Blasco M a (2005) Telomeres and human disease: ageing, cancer and beyond. *Nat Rev Genet* 6(8):611–22.
99. Hanahan D, Weinberg R a (2011) Hallmarks of cancer: the next generation. *Cell* 144(5):646–74.

100. Kim NW, et al. (1994) Specific association of human telomerase activity with immortal cells and cancer. *Science* 266(5193):2011–5.
101. Counter CM, et al. (1992) Telomere shortening associated with chromosome instability is arrested in immortal cells which express telomerase activity. *EMBO J* 11(5):1921–9.
102. Counter CM, et al. (1998) Dissociation among in vitro telomerase activity, telomere maintenance, and cellular immortalization. *Proc Natl Acad Sci* 95(25):14723–8.
103. Hahn WC, et al. (1999) Creation of human tumour cells with defined genetic elements. *Nature* 400(6743):464–8.
104. Hahn WC, et al. (1999) Inhibition of telomerase limits the growth of human cancer cells. *Nat Med* 5(10):1164–70.
105. Henson JD, et al. (2005) A Robust Assay for Alternative Lengthening of Telomeres in Tumors Shows the Significance of Alternative Lengthening of Telomeres in Sarcomas and Astrocytomas. *Clin Cancer Res* 11:217–225.
106. Lundblad V, Blackburn EH (1993) An Alternative Pathway for Yeast Telomere Maintenance Rescues estl- Senescence. *Cell* 73:347–360.
107. McEachern MJ, Blackburn EH (1995) Runaway telomere elongation caused by telomerase RNA gene mutations. *Nature* 376:403–409.
108. Bryan TM, Englezou a, Gupta J, Bacchetti S, Reddel RR (1995) Telomere elongation in immortal human cells without detectable telomerase activity. *EMBO J* 14(17):4240–8.
109. Dunham M a, Neumann a a, Fasching CL, Reddel RR (2000) Telomere maintenance by recombination in human cells. *Nat Genet* 26(4):447–50.
110. Bailey SM, Brenneman M a, Goodwin EH (2004) Frequent recombination in telomeric DNA may extend the proliferative life of telomerase-negative cells. *Nucleic Acids Res* 32(12):3743–51.
111. Muntoni A, Neumann A a, Hills M, Reddel RR (2009) Telomere elongation involves intra-molecular DNA replication in cells utilizing alternative lengthening of telomeres. *Hum Mol Genet* 18(6):1017–27.
112. Wang RC, Smogorzewska A, de Lange T (2004) Homologous recombination generates T-loop-sized deletions at human telomeres. *Cell* 119(3):355–68.
113. Murnane JP, Sabatier L, Marder B a, Morgan WF (1994) Telomere dynamics in an immortal human cell line. *EMBO J* 13(20):4953–62.

114. Henson JD, Neumann AA, Yeager TR, Reddel RR (2002) Alternative lengthening of telomeres in mammalian cells. *Oncogene* 21:598–610.
115. Yeager TR, et al. (1999) Telomerase-negative Immortalized Human Cells Contain a Novel Type of Promyelocytic Leukemia (PML) Body. *Cancer Res* 59:4175–4179.
116. Lee M, et al. (2013) Telomere extension by telomerase and ALT generates variant repeats by mechanistically distinct processes. *Nucleic Acids Res*:1–14.
117. Cesare AJ, et al. (2009) Spontaneous occurrence of telomeric DNA damage response in the absence of chromosome fusions. *Nat Struct Mol Biol* 16(12):1244–51.
118. Cesare AJ, Reddel RR (2010) Alternative lengthening of telomeres: models, mechanisms and implications. *Nat Rev Genet* 11(5):319–30.
119. De Lange T (2005) Shelterin: the protein complex that shapes and safeguards human telomeres. *Genes Dev* 19(18):2100–10.
120. Dejardin J, Kingston RE (2009) Purification of proteins associated with specific genomic loci. *Cell* 136(1):175–186.
121. Baumann P, Cech TR (2001) Pot1, the Putative Telomere End-Binding Protein in Fission Yeast and Humans. *Science* (80-) 292:1171–1175.
122. Loayza D, de Lange T (2003) POT1 as a terminal transducer of TRF1 telomere length control. *Nature* 423:1013–1018.
123. Ye JZ-S, et al. (2004) POT1-interacting protein PIP1: a telomere length regulator that recruits POT1 to the TIN2/TRF1 complex. *Genes Dev* 18(14):1649–54.
124. Kendellen MF, Barrientos KS, Counter CM (2009) POT1 association with TRF2 regulates telomere length. *Mol Cell Biol* 29(20):5611–9.
125. Li G, Eller MS, Firoozabadi R, Gilchrest BA (2003) Evidence that exposure of the telomere 3' overhang sequence induces senescence. *Proc Natl Acad Sci* 100(2):527–31.
126. Yang Q, Zheng Y, Harris CC (2005) POT1 and TRF2 Cooperate To Maintain Telomeric Integrity. *Mol Cell Biol* 25(3):1070–1080.
127. Zaug AJ, Podell ER, Cech TR (2005) Human POT1 disrupts telomeric G-quadruplexes allowing telomerase extension in vitro. *Proc Natl Acad Sci U S A* 102(31):10864–9.
128. He H, et al. (2006) POT1b protects telomeres from end-to-end chromosomal fusions and aberrant homologous recombination. *EMBO J* 25(21):5180–5190.

129. Hockemeyer D, Daniels J-P, Takai H, de Lange T (2006) Recent expansion of the telomeric complex in rodents: Two distinct POT1 proteins protect mouse telomeres. *Cell* 126(1):63–77.
130. Wu L, et al. (2006) Pot1 deficiency initiates DNA damage checkpoint activation and aberrant homologous recombination at telomeres. *Cell* 126:49–62.
131. Palm W, Hockemeyer D, Kibe T, de Lange T (2009) Functional dissection of human and mouse POT1 proteins. *Mol Cell Biol* 29(2):471–82.
132. Baumann P, Price C (2010) Pot1 and telomere maintenance. *FEBS Lett* 584(17):3779–3784.
133. Churikov D, Wei C, Price CM (2006) Vertebrate POT1 restricts G-overhang length and prevents activation of a telomeric DNA damage checkpoint but is dispensable for overhang protection. *Mol Cell Biol* 26(18):6971–82.
134. Murzin AG (1993) OB(oligonucleotide/oligosaccharide binding)-fold: common structural and functional solution for non-homologous sequences. *EMBO J* 12(3):861–867.
135. Lei M, Podell ER, Cech TR (2004) Structure of human POT1 bound to telomeric single-stranded DNA provides a model for chromosome end-protection. *Nat Struct Mol Biol* 11(12):1223–9.
136. Bunch JT, et al. (2005) Distinct requirements for Pot1 in limiting telomere length and maintaining chromosome stability. *Mol Cell Biol* 25(13):5567–78.
137. Karlseder J, Smogorzewska A, de Lange T (2002) Senescence Induced by Altered Telomere State, not Telomere Loss. *Science* (80-) 295:2446–2449.
138. d’Adda di Fagagna F, et al. (2003) A DNA damage checkpoint response in telomere-initiated senescence. *Nature* 426(November):194–198.
139. Herbig U, Jobling WA, Chen BPC, Chen DJ, Sedivy JM (2004) Telomere shortening triggers senescence of human cells through a pathway involving ATM, p53, and p21cip1, but not p16ink4a. *Mol Cell* 14:501–513.
140. Takai H, Smogorzewska A, Lange T De (2003) DNA damage foci at dysfunctional telomeres. *Curr Biol* 13:1549–1556.
141. Flynn RL, et al. (2011) TERRA and hnRNPA1 orchestrate an RPA-to-POT1 switch on telomeric single-stranded DNA. *Nature* 471(7339):532–536.
142. Denchi EL, de Lange T (2007) Protection of telomeres through independent control of ATM and ATR by TRF2 and POT1. *Nature* 448(7157):1068–71.

143. Guo X, et al. (2007) Dysfunctional telomeres activate an ATM-ATR-dependent DNA damage response to suppress tumorigenesis. *EMBO J* 26(22):4709–19.
144. Zou L, Elledge SJ (2003) Sensing DNA damage through ATRIP recognition of RPA-ssDNA complexes. *Science* 300(5625):1542–8.
145. Ray S, Bandaria JN, Qureshi MH, Yildiz A, Balci H (2014) G-quadruplex formation in telomeres enhances POT1/TPP1 protection against RPA binding. *Proc Natl Acad Sci U S A* 111(8):2990–5.
146. Porro A, Feuerhahn S, Reichenbach P, Lingner J (2010) Molecular dissection of telomeric repeat-containing RNA biogenesis unveils the presence of distinct and multiple regulatory pathways. *Mol Cell Biol* 30(20):4808–17.
147. Takai KK, Kibe T, Donigian JR, Frescas D, de Lange T (2011) Telomere protection by TPP1/POT1 requires tethering to TIN2. *Mol Cell* 44(4):647–59.
148. Salas TR, et al. (2006) Human replication protein A unfolds telomeric G-quadruplexes. *Nucleic Acids Res* 34(17):4857–65.
149. Hudson JS, Ding L, Le V, Lewis E, Graves D (2014) Recognition and binding of human telomeric G-quadruplex DNA by unfolding protein 1. *Biochemistry* 53(20):3347–56.
150. Tang J, et al. (2008) G-quadruplex preferentially forms at the very 3' end of vertebrate telomeric DNA. *Nucleic Acids Res* 36(4):1200–8.
151. Wang Q, et al. (2011) G-quadruplex formation at the 3' end of telomere DNA inhibits its extension by telomerase, polymerase and unwinding by helicase. *Nucleic Acids Res* 39(14):6229–37.
152. Colgin LM, Baran K, Baumann P, Cech TR, Reddel RR (2003) Human POT1 Facilitates Telomere Elongation by Telomerase. *Curr Biol* 13:942–946.
153. Armbruster BN, et al. (2004) Rescue of an hTERT Mutant Defective in Telomere Elongation by Fusion with hPot1. *Mol Cell Biol* 24(8):3552–61.
154. Kelleher C, et al. (2005) Human protection of telomeres 1 (POT1) is a negative regulator of telomerase activity in vitro. *Mol Cell Biol* 25(2):808–818.
155. Lei M, Zaug AJ, Podell ER, Cech TR (2005) Switching human telomerase on and off with hPOT1 protein in vitro. *J Biol Chem* 280(21):20449–56.
156. Wang F, et al. (2007) The POT1-TPP1 telomere complex is a telomerase processivity factor. *Nature* 445(7127):506–10.

157. Xin H, et al. (2007) TPP1 is a homologue of ciliate TEBP-beta and interacts with POT1 to recruit telomerase. *Nature* 445(7127):559–62.
158. Latrick CM, Cech TR (2010) POT1–TPP1 enhances telomerase processivity by slowing primer dissociation and aiding translocation. *EMBO J* 29(5):924–933.
159. Miyoshi T, Kanoh J, Saito M, Ishikawa F (2008) Fission yeast Pot1-Tpp1 protects telomeres and regulates telomere length. *Science* 320(5881):1341–4.
160. Zaug AJ, Podell ER, Nandakumar J, Cech TR (2010) Functional interaction between telomere protein TPP1 and telomerase. *Genes Dev* 24:613–622.
161. Hwang H, Buncher N, Opresko PL, Myong S (2012) POT1-TPP1 regulates telomeric overhang structural dynamics. *Structure* 20(11):1872–80.
162. Paeschke K, Simonsson T, Postberg J, Rhodes D, Lipps HJ (2005) Telomere end-binding proteins control the formation of G-quadruplex DNA structures in vivo. *Nat Struct Mol Biol* 12(10):847–54.
163. Sun D, et al. (1997) Inhibition of human telomerase by a G-quadruplex-interactive compound. *J Med Chem* 40(14):2113–6.
164. Rodriguez R, et al. (2008) A Novel Small Molecule That Alters Shelterin Integrity and Triggers a DNA-Damage Response at Telomeres. *J Am Chem Soc* 130(47):15758–15759.
165. Gomez D, et al. (2006) Telomestatin-induced telomere uncapping is modulated by POT1 through G-overhang extension in HT1080 human tumor cells. *J Biol Chem* 281(50):38721–9.
166. Gomez D, et al. (2006) The G-quadruplex ligand telomestatin inhibits POT1 binding to telomeric sequences in vitro and induces GFP-POT1 dissociation from telomeres in human cells. *Cancer Res* 66(14):6908–12.
167. Fry M, Loeb L a. (1999) Human Werner Syndrome DNA Helicase Unwinds Tetrahelical Structures of the Fragile X Syndrome Repeat Sequence d(CGG) n. *J Biol Chem* 274(18):12797–12802.
168. Blanco R, Muñoz P, Flores JM, Klatt P, Blasco MA (2007) Telomerase abrogation dramatically accelerates TRF2-induced epithelial carcinogenesis. *5*:206–220.
169. Crabbe L, Verdun RE, Haggblom CI, Karlseder J (2004) Defective telomere lagging strand synthesis in cells lacking WRN helicase activity. *Science* 306(5703):1951–3.
170. Baran N, Pucshansky L, Marco Y, Benjamin S, Manor H (1997) The SV40 large T-antigen helicase can unwind four stranded DNA structures linked by G-quartets. *Nucleic Acids Res* 25(2):297–303.

171. Hwang H, et al. (2014) Telomeric Overhang Length Determines Structural Dynamics and Accessibility to Telomerase and ALT-Associated Proteins. *Structure* 22(6):842–53.
172. Temime-Smaali N, et al. (2009) The G-quadruplex ligand telomestatin impairs binding of topoisomerase III α to G-quadruplex-forming oligonucleotides and uncaps telomeres in ALT cells. *PLoS One* 4(9):e6919.
173. Koirala D, et al. (2013) Long-loop G-quadruplexes are misfolded population minorities with fast transition kinetics in human telomeric sequences. *J Am Chem Soc* 135:2235–41.
174. Gray RD, Chaires JB (2008) Kinetics and mechanism of K⁺- and Na⁺-induced folding of models of human telomeric DNA into G-quadruplex structures. *Nucleic Acids Res* 36(12):4191–203.
175. Ying L, Green JJ, Li H, Klennerman D, Balasubramanian S (2003) Studies on the structure and dynamics of the human telomeric G quadruplex by single-molecule fluorescence resonance energy transfer. *Proc Natl Acad Sci* 100(25):14629–34.
176. Oganessian L, Moon IK, Bryan TM, Jarstfer MB (2006) Extension of G-quadruplex DNA by ciliate telomerase. *EMBO J* 25(5):1148–59.
177. Harman D (1972) Free radical theory of aging: dietary implications. *Am J Clin Nutr*:839–843.
178. Fraga CG, Shigenaga MK, Park J, Degant P, Amest BN (1990) Oxidative damage to DNA during aging : 8-Hydroxy- 2 ' -deoxyguanosine in rat organ DNA and urine. *Proc Natl Acad Sci* 87(June):4533–4537.
179. Von Zglinicki T (2002) Oxidative stress shortens telomeres. *Trends Biochem Sci* 27(7):339–44.
180. Von Zglinicki T (2000) Role of oxidative stress in telomere length regulation and replicative senescence. *Ann N Y Acad Sci* 908:99–110.
181. Harbo M, Koelvraa S, Serakinci N, Bendix L (2012) Telomere dynamics in human mesenchymal stem cells after exposure to acute oxidative stress. *DNA Repair (Amst)* 11(9):774–9.
182. Vallabhaneni H, O'Callaghan N, Sidorova J, Liu Y (2013) Defective repair of oxidative base lesions by the DNA glycosylase Nth1 associates with multiple telomere defects. *PLoS Genet* 9(7):e1003639.
183. Duan J, Duan J, Zhang Z, Tong T (2005) Irreversible cellular senescence induced by prolonged exposure to H₂O₂ involves DNA-damage-and-repair genes and telomere shortening. *Int J Biochem Cell Biol* 37(7):1407–20.

184. Hewitt G, et al. (2012) Telomeres are favoured targets of a persistent DNA damage response in ageing and stress-induced senescence. *Nat Commun* 3(708):1–9.
185. Von Zglinicki T, Saretzki G, Docke W, Lotze C (1995) Mild hyperoxia shortens telomeres and inhibits proliferation of fibroblasts: a model for senescence? *Exp Cell Res* 220:186–193.
186. Petersen S, Saretzki G, von Zglinicki T (1998) Preferential accumulation of single-stranded regions in telomeres of human fibroblasts. *Exp Cell Res* 239(1):152–60.
187. Furumoto K, Inoue E, Nagao N, Hiyama E, Miwa N (1998) Age-dependent telomere shortening is slowed down by enrichment of intracellular vitamin C via suppression of oxidative stress. *Life Sci* 63(11):935–948.
188. Brandl A, et al. (2011) Oxidative stress induces senescence in chondrocytes. *J Orthop Res* 29(7):1114–20.
189. Rhee DB, Ghosh A, Lu J, Bohr V a, Liu Y (2011) Factors that influence telomeric oxidative base damage and repair by DNA glycosylase OGG1. *DNA Repair (Amst)* 10(1):34–44.
190. Theruvathu J a, Darwanto A, Hsu CW, Sowers LC (2014) The effect of Pot1 binding on the repair of thymine analogs in a telomeric DNA sequence. *Nucleic Acids Res* 42(14):9063–9073.
191. Gorbunova V, Seluanov A, Pereira-Smith OM (2002) Expression of human telomerase (hTERT) does not prevent stress-induced senescence in normal human fibroblasts but protects the cells from stress-induced apoptosis and necrosis. *J Biol Chem* 277(41):38540–9.
192. Forsyth NR, Evans a. P, Shay JW, Wright WE (2003) Developmental differences in the immortalization of lung fibroblasts by telomerase. *Aging Cell* 2(5):235–243.
193. Kovalenko O a, et al. (2010) A mutant telomerase defective in nuclear-cytoplasmic shuttling fails to immortalize cells and is associated with mitochondrial dysfunction. *Aging Cell* 9(2):203–19.
194. Hegde ML, Hazra TK, Mitra S (2008) Early steps in the DNA base excision/single-strand interruption repair pathway in mammalian cells. *Cell Res* 18(1):27–47.
195. Evans MD, Cooke MS (2004) Factors contributing to the outcome of oxidative damage to nucleic acids. *Bioessays* 26(5):533–42.
196. Zhou J, Liu M, Fleming AM, Burrows CJ, Wallace SS (2013) Neil3 and NEIL1 DNA glycosylases remove oxidative damages from quadruplex DNA and exhibit preferences for lesions in the telomeric sequence context. *J Biol Chem* 288(38):27263–72.

197. Oikawa S, Tada-Oikawa S, Kawanishi S (2001) Site-specific DNA damage at the GGG sequence by UVA involves acceleration of telomere shortening. *Biochemistry* 40(15):4763–8.
198. Vorlíčková M, Tomasko M, Sagi AJ, Bednarova K, Sagi J (2012) 8-oxoguanine in a quadruplex of the human telomere DNA sequence. *FEBS J* 279(1):29–39.
199. Wang Z, et al. (2010) Characterization of oxidative guanine damage and repair in mammalian telomeres. *PLoS Genet* 6(5):e1000951.
200. Opresko PL, Fan J, Danzy S, Wilson DM, Bohr V a (2005) Oxidative damage in telomeric DNA disrupts recognition by TRF1 and TRF2. *Nucleic Acids Res* 33(4):1230–9.
201. Ghosh A, Rossi ML, Aulds J, Croteau D, Bohr V a (2009) Telomeric D-loops containing 8-oxo-2'-deoxyguanosine are preferred substrates for Werner and Bloom syndrome helicases and are bound by POT1. *J Biol Chem* 284(45):31074–84.
202. Shibutani S, Takeshita M, Grollman AP (1991) Insertion of specific bases during DNA synthesis past the oxidation-damaged base 8-oxodG. *Nature* 349:431–434.
203. Szalai V a, Singer MJ, Thorp HH (2002) Site-specific probing of oxidative reactivity and telomerase function using 7,8-dihydro-8-oxoguanine in telomeric DNA. *J Am Chem Soc* 124(8):1625–31.
204. Clark DW, Phang T, Edwards MG, Geraci MW, Gillespie MN (2012) Promoter G-quadruplex sequences are targets for base oxidation and strand cleavage during hypoxia-induced transcription. *Free Radic Biol Med* 53(1):51–9.
205. Stebbeds WJD, Lunec J, Larcombe LD (2012) An in silico study of the differential effect of oxidation on two biologically relevant G-quadruplexes: possible implications in oncogene expression. *PLoS One* 7(8):e43735.
206. Lee JY, Kim DS (2009) Dramatic effect of single-base mutation on the conformational dynamics of human telomeric G-quadruplex. *Nucleic Acids Res* 37(11):3625–34.
207. Tomasko M, Vorlíčková M, Sagi J (2009) Substitution of adenine for guanine in the quadruplex-forming human telomere DNA sequence G(3)(T(2)AG(3))(3). *Biochimie* 91(2):171–9.
208. Sagi J, Renciuik D, Tomasko M, Vorlíčková M (2010) Quadruplexes of human telomere DNA analogs designed to contain G:A:G:A, G:G:A:A, and A:A:A:A tetrads. *Biopolymers* 93(10):880–6.
209. Skoláková P, Bednářová K, Vorlíčková M, Sagi J (2010) Quadruplexes of human telomere dG(3)(TTAG(3))(3) sequences containing guanine abasic sites. *Biochem Biophys Res Commun* 399(2):203–8.

210. Ha T, et al. (1996) Probing the interaction between two single molecules: Fluorescence resonance energy transfer between a single donor and a single acceptor. *Proc Natl Acad Sci* 93:6264–6268.
211. Roy R, Hohng S, Ha T (2008) A practical guide to single-molecule FRET. *Nat Methods* 5(6):507–516.
212. Joo C, Balci H, Ishitsuka Y, Buranachai C, Ha T (2008) Advances in single-molecule fluorescence methods for molecular biology. *Annu Rev Biochem* 77:51–76.
213. Sowd G, Lei M, Opresko PL (2008) Mechanism and substrate specificity of telomeric protein POT1 stimulation of the Werner syndrome helicase. *Nucleic Acids Res* 36(13):4242–56.
214. Riou JF, et al. (2002) Cell senescence and telomere shortening induced by a new series of specific G-quadruplex DNA ligands. *Proc Natl Acad Sci* 99(5):2672–7.
215. Tahara H, et al. (2006) G-Quadruplex stabilization by telomestatin induces TRF2 protein dissociation from telomeres and anaphase bridge formation accompanied by loss of the 3' telomeric overhang in cancer cells. *Oncogene* 25(13):1955–66.
216. Tauchi T, et al. (2006) Telomerase inhibition with a novel G-quadruplex-interactive agent, telomestatin: in vitro and in vivo studies in acute leukemia. *Oncogene* 25(42):5719–25.
217. Phatak P, et al. (2007) Telomere uncapping by the G-quadruplex ligand RHPS4 inhibits clonogenic tumour cell growth in vitro and in vivo consistent with a cancer stem cell targeting mechanism. *Br J Cancer* 96(8):1223–33.
218. Burger AM, et al. (2005) The G-Quadruplex-Interactive Molecule BRACO-19 Inhibits Tumor Growth, Consistent with Telomere Targeting and Interference with Telomerase Function. *Cancer Res* 65:1489–1496.
219. Li J, et al. (2001) Inhibition of the Bloom's and Werner's syndrome helicases by G-Quadruplex interacting ligands. *Biochemistry* 40:15194–15202.
220. Gomez D, et al. (2004) Interaction of telomestatin with the telomeric single-strand overhang. *J Biol Chem* 279(40):41487–94.
221. Herbert B, et al. (1999) Inhibition of human telomerase in immortal human cells leads to progressive telomere shortening and cell death. *Proc Natl Acad Sci U S A* 96(25):14276–81.
222. De Cian A, et al. (2007) Reevaluation of telomerase inhibition by quadruplex ligands and their mechanisms of action. *Proc Natl Acad Sci U S A* 104(44):17347–52.